FZD-536

Application of the Master Curve Approach to Fracture Mechanics Characterisation of Reactor Pressure Vessel Steel

Hans-Werner Viehrig, Conrad Zurbuchen,
Hans-Jakob Schindler, Dietmar Kalkhof

Juni 2010

Wissenschaftlich-Technische Berichte
FZD-536 2010 · ISSN 1437-322X

WISSENSCHAFTLICH-TECHNISCHE BERICHTE

Forschungszentrum
Dresden Rossendorf

Wissenschaftlich-Technische Berichte
FZD-536
Juni 2010

Hans-Werner Viehrig, Conrad Zurbuchen
Hans-Jakob Schindler, Dietmar Kalkhof

Application of the Master Curve Approach to Fracture Mechanics Characterisation of Reactor Pressure Vessel Steel

Forschungszentrum
Dresden Rossendorf

Application of the Master Curve Approach to Fracture Mechanics Characterisation of Reactor Pressure Vessel Steel

Hans-Werner Viehrig*, Conrad Zurbuchen**, Hans-Jakob Schindler*** and Dietmar Kalkhof****

* Forschungszentrum Dresden-Rossendorf, P.O.Box 01314 Dresden, Germany
** TU Dresden, Fakultät Maschinenwesen, Institut für Werkstoffwissenschaft, 01062 Dresden, Germany
*** Mat-Tec AG, Unterer Graben 27, 8401 Winterthur, Switzerland
**** Swiss Federal Nuclear Safety Inspectorate ENSI, Industriestrasse 19, 5200 Brugg, Switzerland

Abstract

The paper presents results of a research project founded by the Swiss Federal Nuclear Inspectorate (No. H100456) concerning the application of the Master Curve approach in nuclear reactor pressure vessels integrity assessment. The main focus is put on the applicability of pre-cracked 0.4T-SE(B) specimens with short cracks, the verification of transferability of MC reference temperatures T_0 from 0.4T thick specimens to larger specimens, ascertaining the influence of the specimen type and the test temperature on T_0, investigation of the applicability of specimens with electroerosive notches for the fracture toughness testing, and the quantification of the loading rate and specimen type on T_0. The test material is a forged ring of steel 22 NiMoCr 3-7 of the uncommissioned German pressurized water reactor Biblis C.
SE(B) specimens with different overall sizes (specimen thickness B=0.4T, 0.8T, 1.6T, 3T, fatigue pre-cracked to a/W=0.5 and 20% side-grooved) have comparable T_0. T_0 varies within the 1σ scatter band. The testing of C(T) specimens results in higher T_0 compared to SE(B) specimens. It can be stated that except for the lowest test temperature allowed by ASTM E1921-09a, the T_0 values evaluated with specimens tested at different test temperatures are consistent. The testing in the temperature range of T_0 ± 20 K is recommended because it gave the highest accuracy. Specimens with a/W=0.3 and a/W=0.5 crack length ratios yield comparable T_0. The T_0 of EDM notched specimens lie 41 K up to 54 K below the T_0 of fatigue pre-cracked specimens. A significant influence of the loading rate on the MC T_0 was observed. The HSK AN 425 test procedure is a suitable method to evaluate dynamic MC tests. The reference temperature T_0 is eligible to define a reference temperature RT_{To} for the ASME-K_{IC} reference curve as recommended in the ASME Code Case N-629. An additional margin has to be defined for the specific type of transient to be considered in the RPV integrity assessment. This margin also takes into account the level of available information of the RPV to be assessed.

Content

1. Introduction

Present codes for the integrity assessment of Nuclear Power Plant (NPP) reactor pressure vessels (RPV) use an indirect and correlative approach of determining the fracture toughness of the RPV steels in the initial and irradiated condition. Procedures applied in the different countries vary in the details, but are based on the same principle. In general these procedures use results of Charpy V-notch and drop weight testing to determine the reference temperature, RT_{NDT}, for a fracture toughness, K_{IC}, reference curve. The reference fracture toughness curve is based on an empirical analysis of the relationship between measured RT_{NDT} and K_{IC} values and is considered to be adequately conservative. Most of the codes in different countries are based on the ASME reference curve [ASME NB-2300], whose shape though empirically derived from different RPV steels (base and weld metals) of ASTM type, but reflects only one specific material, the "HSST 02 plate". This concept has the following disadvantages:

- It is not consistent since it links fracture mechanical and technological parameters and
- Margins of safety and probability estimation cannot be quantified.

The Master Curve (MC) approach [Mc Cabe-2005] as adopted in the standard test method ASTM E1921 characterises the fracture toughness of ferritic steels. This approach is more naturally suited to probabilistic analyses because it defines both a mean transition toughness value and a distribution around that value. It is reasonable to expect that in the future the determination of nuclear power plant (NPP) operating limits will be based on Master Curve methodology [Brumovsky-2001, Rosinski-2000, 2004, Server-2005a, 2005b, 2009]. The need to assess RPV fracture toughness more accurately will drive the authorities to demand the use of modified surveillance specimens to measure MC fracture toughness, in addition to the present indirect and correlative approaches. However, there are still some open questions. Some peculiar features of T_0 are not yet fully understood.

The Swiss Federal Nuclear Safety Inspectorate (ENSI) initiated and funded a research project (No. H-100456) to investigate open questions connected with the application of the MC approach in the RPV integrity assessment. This paper presents results of the research project which investigated different influencing variables such as specimen type and size, crack length ratio and crack geometry on the MC based reference temperature T_0. Another main point is the influence of the loading rate on T_0. The standard MC approach standardised in ASTM E1921 is defined for quasi-static loading conditions. In the latest version of Test Standard ASTM E1921-09a loading rates are restricted to 0.1 $MPa\sqrt{m}/s \leq dK/dt \leq 2$ $MPa\sqrt{m}/s$. However, the use of the MC method for dynamic tests is obvious even if dynamic values have limited application in the RPV integrity assessment. The loading rates in any actual RPV operating or accident conditions are not dynamic. Nevertheless, knowledge of the loading rate dependence of T_0 is useful, because many of the plants operating heat-up and cool-down curves based on a reference fracture toughness curve (such as ASME Code K_{IR} curve) which in turn is based on the combination of crack arrest and dynamic fracture toughness. Master Curve reference temperature is known to be highly affected by loading rate. A Swiss Test guideline draft (HSK-AN-425 Rev 5) about dynamic fracture toughness testing was checked. It outlines the testing of side-grooved Charpy-size specimens and their evaluation according to the Master Curve concept.

The tests were performed on a German type 22 NiMoCr 3 7 reactor pressure vessel (RPV) steel.

2. Basics of the Master Curve Approach

Since all aims of the research project are closely related to the Master Curve approach, the most important fundamentals of this method will be outlined before explaining the individual aims in section 3. The MC approach examines the cleavage failure of a specimen in the lower ductile-to-brittle transition range. It comprises the following basic assumptions:

- the fracture probability cleavage model (Weibull statistics),

- the prediction of the influence of the specimen size on the failure probability, i.e. specimen thickness adjusted to 1T (25.4 mm) and
- an universal temperature dependence of cumulative fracture probability.

2.1 Fracture probability cleavage model

The standard Master Curve cumulative failure probability expression is of the form:

$$P_f = 1 - \exp\left\{ \frac{B}{B_0} \cdot \left(\frac{K_{Jc} - K_{min}}{K_0 - K_{min}} \right)^4 \right\} \tag{1}$$

2.2 Specimen size adjustment (1T)

The MC approach enables the comparison of fracture toughness values, K_{Jc}, measured on specimens with different thicknesses. This is possible through a normalizing procedure in which for every data set all individual fracture toughness K_{Jc} values are converted to corresponding fracture toughness values, $K_{Jc(1T)}$, of a fictitious specimen thickness of B = 1T = 25.4 mm, Eq. (2). The statistical weakest-link theory is used to model the effect of specimen size on the failure probability in the ductile-to-brittle transition range.

$$K_{Jc(1T)} = K_{min} + (K_{Jc} - K_{min}) \cdot \left(\frac{B}{B_{1T}} \right)^{1/4} \tag{2}$$

For the calculation of T_0 specimen-thickness adjusted $K_{Jc(1T)}$ values are used as the input.

2.3 Universal temperature dependence of cumulative fracture probability

The Master Curve is an empirically derived universal transition range curve of fixed shape for statistic cleavage fracture toughness versus temperature. Eq. (3) expresses the scale parameter K_0 (63.2 percentile level), and Eq. (4) the median (50%) cumulative fracture probability $K_{Jc(med)1T}$.

$$K_0 = 31 + 77 \cdot \exp\{0.019 \cdot (T - T_0)\} \tag{3}$$

$$K_{Jc(med)1T} = 30 + 70 \cdot \exp(0.019 \cdot (T - T_0)) \tag{4}$$

2.4. Testing and evaluation procedure

The specimens were loaded until they failed by cleavage instability. The J-integral values at instability (J_c, "c" denoting failure by cleavage) are converted into their equivalents, K_{Jc} (fracture toughness at onset of cleavage initiation), Eq. (5), assuming plane strain for elastic modulus, E:

$$K_{Jc} = \sqrt{J_c \cdot \frac{E}{(1 - \nu^2)}} \tag{5}$$

Before solving for T_0, a number of censoring steps have to be applied. Firstly, all data sets that did not fail in cleavage mode are discarded. Secondly, all data violating the specimen size validity criterion (maximum K_{Jc} measuring capacity of the concerned specimen, $K_{Jc(limit)}$) of Eq. (6) are censored on the toughness value corresponding to the validity criteria $K_{Jc(limit)}$.

$$K_{Jc(limit)} \leq \sqrt{\frac{b \cdot \sigma_{YS} \cdot E}{M \cdot (1 - \nu^2)}} \tag{6}$$

The value of T_0 is calculated according to the test standard ASTM E1921-09a using single or multitemperature methods:
Single temperature evaluation:

Evaluation of the scale parameter K_0 is performed according to Eq. (7) using individual cleavage fracture toughness values $K_{Jc(1T)}$ measured at one test temperature. Eq. (8) gives the median cumulative probability of fracture $K_{Jc(med)1T}$ of the data set, which is used to calculate T_0 at $K_{Jc(med)1T}$ of 100 MPa√m according to Eq. (9).

$$K_0 = \left[\sum_{i=1}^{N} \frac{\left(K_{Jc(i)} - K_{min}\right)^4}{N} \right]^{1/4} + K_{min} \quad (7)$$

If invalid or censored values (Eq. (6)) occur N is replaced by the number of valid values, r.

$$K_{Jc(med)1T} = K_{min} + \left(K_0 - K_{min}\right) \cdot \left(\ln 2\right)^{1/4} \quad (8)$$

$$T_0 = T - \left(\frac{1}{0.019}\right) \cdot \ln\left(\frac{K_{Jc(med)1T} - 30}{70}\right) \quad (9)$$

Multitemperature evaluation:
The multi-temperature option of ASTM E1921-09a offers a tool for the calculation of T_0 with $K_{Jc(1T)}$ data measured at different temperatures by an iterative solution of Eq. (10):

$$\sum_{i=1}^{n} \frac{\delta_i \cdot \exp\{0.019 \cdot [T_i - T_0]\}}{11 + 77 \cdot \exp\{0.019 \cdot [T_i - T_0]\}} - \sum_{i=1}^{n} \frac{\left(K_{Jc(i)} - 20\right)^4 \cdot \exp\{0.019 \cdot [T_i - T_0]\}}{\left(11 + 77 \cdot \exp\{0.019 \cdot [T_i - T_0]\}\right)^5} = 0 \quad (10)$$

ASTM E1921-09a stipulates validity criteria for T_0 determination. Following weighting system specifies the required minimum of valid K_{Jc} data points:

$$\sum_{i=1}^{3} r_i n_i \geq 1 \quad (11)$$

To fulfil the weighting sum requirement in Eq. (11), at least the requisite minimum number of six test samples are tested, but usually more, depending on the choice of test temperature and the number of censored specimens. Therefore, testing continues until at least the minimum number of valid test data was achieved. The allowed test temperature range in ASTM E1921-09a is T_0 ± 50 K. It is recommends that the specimens should be tested in this range and as close as possible to the T_0 to maximize the accuracy in the measurement.

2.5 Application of the Master Curve Approach in Reactor Pressure Vessel Integrity Assessment

There is a short-range and a long-range objective in the introduction of the MC approach in the NPP RPV integrity assessment [Rosinski-2000]. In the near future, the intention is to use the alternative reference temperature without losing the historical link to the fracture data that was the basis of the K_{Ic} reference curves. The shape of the universal ASME reference curve Eq. (12) was empirically derived from different RPV steels (base and weld metals) of ASTM type, but it reflects one specific material, the "HSST 02 plate".

$$K_{Ic} = 36.5 + 22.783 \cdot \exp\left[0.036 \cdot \left(T - RT_{T_0}\right)\right] \quad (12)$$

In the United States the direct approach has been implemented in the ASME Code Case N-629 "Use of Fracture Toughness Test Data to Establish Reference Temperature for Pressure Retaining Materials for Section XI" [ASME N-629]. This new parameter is termed RT_{T0} and given by Eq. (13).

$$RT_{T_0} = T_0 + 35F\ (19.4K) \quad (13)$$

The additional temperature increment in Eq. (13) was established to account for uncertainties and the general scatter in the measured fracture toughness data. In order to

provide an objective evaluation of the proposed alternative reference temperature, standards of acceptability must be determined. The ASME K_{IC} curve indexed with RT_{To} must continue to appropriately envelop the measured fracture toughness data. In establishing RT_{To} definition it has been tried to maintain consistency between how well a RT_{NDT}- and RT_{To}-indexed ASME K_{Ic} reference curve envelop the K_{IC} values of the original ASME dataset [Rosinski-1999, Server-2000]. The RT_{To}-indexed ASME K_{Ic} reference curve is approximately equivalent to the MC for 5% fracture probability. However, the 5% MC and the ASME K_{IC} reference curve have slightly different shapes. Therefore, any definition of RT_{To} implies an intersection point of the two curves at a fracture toughness of 151 MPa√m. Below this toughness value the ASME K_{IC} reference curve would be expected to envelop more the 95% of the 1T toughness data and vice versa.
The MC approach is based on an understanding of the statistics of cleavage failure of a specimen that was not available when the ASME K_{Ic} reference curve was developed. The statistical size effect as treated with Eq. (2) is a significant departure from traditional linear elastic fracture mechanics, where the toughness transition data are held to be size-invariant material property values. The test standard ASTM E399-09 now does not apply to specimens of ferritic steels which fail by cleavage fracture in the ductile-to-brittle transition region, where the crack front length affects the measurement in a stochastic manner independent of crack front constraint. Here it is referred to the test standard ASTM E1921.
The benefit of ASME Code Case N-629 is that both the reference temperature for the unirradiated and irradiated state is related to a fracture mechanics parameter which can be measured on unirradiated and irradiated specimens, respectively. The ASME RT_{T0} has also been adopted in the RPV integrity assessment codes of countries outside the USA. For RPV integrity assessment regulatory bodies add additional margins to consider uncertainties as [Server-2005a]:

$$M = Y\sqrt{\sigma_{T_0}^2 + \sigma_{\phi t}^2 + \sigma_{HT}^2 + \cdots} \tag{14}$$

Y safety factor in the margin term
σ_{To} uncertainty in the reference temperature T_0 in K
$\sigma_{\phi t}$ uncertainty in the neutron fluence in K
σ_{HT} uncertainty in material heat treatement (non-homogeneity) in K

The selection of the factor Y depends upon integrity assessment requirements. In many engineering applications, a value for Y of two is typical since it represents an approximate 95% confidence level. However, the safety margin depends on the level of information available. In Germany for example, RT_{To} is adopted in the Nuclear Safety Standards Commission Rule KTA 3203 version 6/01 “Surveillance of the Irradiation Behaviour of Reactor Pressure Vessel Materials of LWR Facilities” [KTA 3203]. The draft of the Swiss Federal Nuclear Safety Inspectorate (ENSI) guideline ENSI-B01/d [ENSI-2010] recommends the following T_0 based reference temperatures:

- RT_X with T_0 measured on Charpy size SE(B) specimens: $RT_X = T_0 + 55K$ (15)
- RT_X with T_0 measured on 1T-C(T) specimens: $RT_X = T_0 + 40K$ (16)

The long-range objective is to apply the statistically defined MC in place of the current code reference fracture toughness curves. The MC allows predictions of the failure of a specimen on the basis of failure probabilities. For the integrity assessment, the selection of an appropriate lower confidence bound (X) needs to be made. The “Unified Procedure for Lifetime Assessment of Component and Piping in WWER NPPs - VERLIFE” [VERLIFE-2003] applies directly the MC for 5% fracture probability according to ASTM E1921 (Eq. (17) as fracture toughness reference curve.

$$K_{Jc}^{5\%}(T) = \min\{25.2 + 36.6 \cdot \exp[0.019 \cdot (T - RT_0)]; 200\} \quad MPa\sqrt{m} \tag{17}$$

A reference temperature, RT_0, is defined as:

$$RT_0 = T_0 + \sigma \tag{18}$$

3. Aims of the research project

3.1 Influence of specimen size

It has to be examined whether the small Charpy-size 0.4T single-edge bend (SE(B)-) specimens yield the same T_0 as larger specimens.
Regarding the absolute specimen size no limitations are made in ASTM E1921 as long as the geometry ratios W/B/L as shown in Figure 4.2 are kept. However, the specimen shall not be too small, because the remaining ligament shall possess a certain minimum length to ensure the constraint in front of the crack at fracture (Eq. (6); ASTM E1921-09a, §7.5).
Therefore, provided the 1T conversion formula Eq. (2) of ASTM E1921 is correct, the T_0 of the applied different SE(B) specimen sizes B=0.4T, 0.8T, 1.6T und 3T should be essentially the same, taking into account the 1σ standard deviation. Figure 3.1 shows broken halves of the tested SE(B) specimens of different sizes as well as 1T-C(T) specimen.

Fig. 3.1: Halves of the tested SE(B) specimens with B=0.4T, 0.8T, 1.6T and 3T as well as a 1T-C(T) specimen.

3.2 Influence of specimen type on MC reference temperature T_0

A well-known factor affecting T_0 is the specimen type. Most MC tests exhibit a bias in T_0 of 10 to 15 K between 0.4T-SE(B) specimens and 1T-C(T) specimens, in which SE(B) specimens yield higher T_0, thus being less conservative. This bias is mentioned in the Standard ASTM E1921-09a, but with no clear explanation. The exact reason for this effect seems to be not been fully understood yet, although lots of research efforts are spent on this question often it is attributed to a faster loss of constraint in the small 0.4T-SE(B) specimens compared with 1T thick C(T) specimens, thus fracturing earlier, at lower fracture toughness values K_{Jc}, which is reflected in a higher T_0.

3.3 Influence of the test temperature on reference temperature T_0

3.4 Influence of crack length ratio a/W on T_0

Fracture mechanics testing is usually carried out on Charpy-size single-edge bend (SE(B)-) specimens with a crack length-to-width ratio of a/W=0.5 (deep cracks). This assures that the constraint at the crack tip is saturated. However, decades ago, the Swiss first generation nuclear power plants Gösgen and Leibstadt were equipped with surveillance specimens with shorter crack length ratios of a/W=0.3 (short crack). Therefore, besides testing sets of standard specimens with a/W=0.5, all tests were also performed on short crack specimens a/W=0.3 in order to investigate quantitatively the effect of the crack length on fracture toughness or T_0, respectively.

3.5 Replacement of fatigue cracks by electroerosive notches

According to common fracture toughness test standards like ASTM E1921 or ASTM E1820 the specimens shall be fatigue pre-cracked prior to testing. In contrast, electroerosive (EDM) notches have a blunter crack-tip of a finite radius. Using an EDM wire of 0.1 mm thickness, we obtained slits of 0.12 mm width. EDM notching of a specimen instead of fatigue pre-cracking offers a number of advantages. Firstly, it is faster because it permits batch processing. Secondly, EDM reliably produces 5.00 mm long, perfectly straight cracks all along the crack front in contrast to pre-cracked crack fronts which are usually curved, being >5mm in the centre region and <5mm in the surface regions. Thirdly, EDM provides a convenient means to pre-crack neutron embrittled specimens. This is sometimes necessary for older specimens with no or too short pre-cracks which need (re-)pre-cracking to the desired a/W ratio. Embrittled steel is very sensitive and at times cracks in a brittle mode even at the very low fatigue pre-cracking loads prior to the actual testing. Fourthly, EDM notching can be helpful in preparing specimens of inhomogeneous structure such as welding seams [Viehrig-09a]. EDM allows to place the crack tip exactly in the desired location of the heat affected zone or a welding bead of a multilayer welding seam. Therefore, in order to verify whether fatigue pre-cracks might be replaced by EDM notches in such cases, tests were performed not only on fatigue pre-cracked specimens but also on EDM notched specimens.

3.6 Influence of loading rate on T_0 (quasi-static vs. dynamic)

The tests standard ASTM E1921 is originally elaborated for quasi-static testing with loading rates in the range of 0.1 to 2 MPa√m/s. The latest version of ASTM E1921-09a now allows higher loading rates. It is well known that the loading rate is one of the most influencing parameter on fracture toughness in the ductile-to-brittle transition range. Correspondingly, it has a strong effect on T_0 [Joyce-98; Yoon-02; Viehrig-2002; Server-2009]. ENSI Guideline HSK-AN-425 proposes MC testing at higher loading rates (instrumented impact tests), suggesting MC evaluation algorithms for such data. To verify the HSK-AN-425 results, another approach was developed in which first the dynamic J_{cd} is evaluated according to ISO/FDIS 26843 “Metallic materials -- Measurement of fracture toughness of steels at impact loading rates using precracked Charpy specimens”, and these values are fed into the standard Master Curve Evaluation Method ASTM E1921-09.
A number of problems occur under impact testing, particularly when testing small 0.4T-SE(B) specimens for the evaluation according to ASTM E1921-09a. High loading rates introduce large amplitude oscillations, which increase the error in the measured force. A certain minimum velocity is given by the requirement that the kinetic energy provided by the hammer should be higher than about three times the fracture energy of the specimen. The upper limit of the resulting fracture toughness is given by the specimen size validity criteria in Eq. (6). The window of the loading rate range complying all requirements was found to be narrow.

4. Material and specimens

4.1 Material

The specimens were machined from the sections of a reactor pressure vessel (RPV) forged ring of steel 22 NiMoCr 3-7 of the uncommissioned German pressurized water reactor Biblis C. The lower ring has been selected as one of the test materials in EU funded research programmes such as CASTOC [CASTOC-04] because it is representative of many modern Western light water reactor RPV manufactured after 1970.

4.2 Specimen machining and preparation

The RPV vessel and the sampling region are shown in Figure 4.1. From this lower forged ring two large blocks were cut. The complete cutting scheme of one of them is shown in Fig. 4.2. The inner surface of the vessel was cladded with austenitic steel. Each of the two blocks was first cut into a longer section from which the four large 3T-SE(B) specimens were machined, and into a squarish section from which the other specimens like cylindrical B8x40 tensile specimens, Charpy-V specimens, 0.4T-SE(B) specimens and 1T-C(T) specimens were machined. The 1.6T-SE(B) specimens were not directly machined from the blocks, but extracted from broken halves of 3T-SE(B) specimens to exclude a possible influence of sampling location on the test results. Likewise, the 0.8T-SE(B) specimens were machined from broken halves of 1.6T- and 3T-SE(B) specimens. Table 4.1 summarises the number and types of the machined specimens.
To ensure that all specimens' crack fronts lie within the inner 2/3 of the wall thickness as prescribed by ENSI codes, a layer of 1/6 of the thickness was cut off from either side of the blocks, including the cladding (Fig 4.2).

Table 4.1: Number, type and codes of specimens

Number	Type
30	cylindrical tensile specimens B8x40
30	Charpy-V specimens for impact tests
36	1T-C(T) specimens, 20% side-grooved
9	0.5T-C(T) specimens, 20% side-grooved
4	3T-SE(B) specimens
16	1.6T-SE(B) specimens (from 3T-SE(B) specimens)
12	0.8T-SE(B) specimens (from 1.6T-SE(B) specimens)
24	0.8T-SE(B) specimens (from 3T-SE(B) specimen halves CR, CL, DR)
107	0.4T-SE(B) specimens with a/W=0.5
75	0.4T-SE(B) specimens with a/W=0.3 from specimen half DR of the 3T-SE(B) specimen D
334	Total

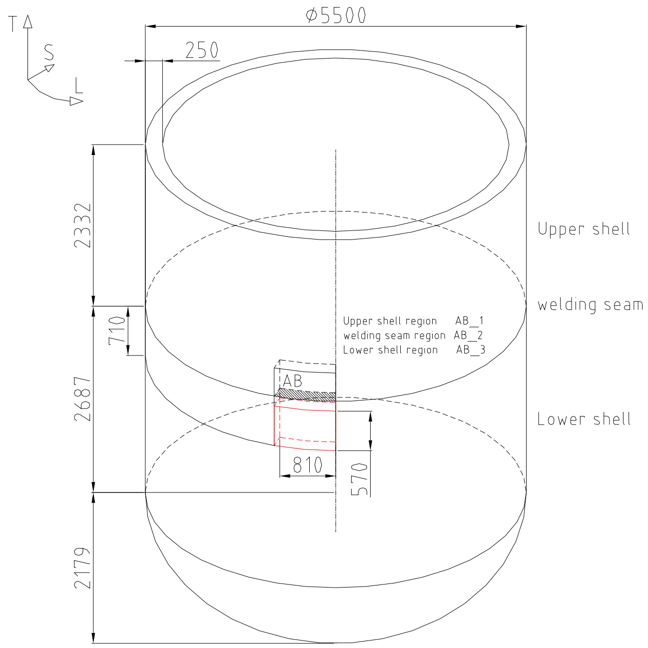

Figure 4.1: RPV vessel geometry, the sampling region is shaded red [Ritter-2002]

All SE(B) and C(T) specimens have the same orientation (T-S according to [ASTM E 1823] and X-Z according to [ISO 3785]). The SE(B) specimens have a W/B ratio of 1:1 and crack length ratios a/W of 0.3 and 0.5. Specimen thickness values (without side-grooves) were B=0.4T, 0.8T, 1.6T and 3T (Fig. 3.1). The C(T) specimens have W/B ratio of 2:1 and crack length ratio a/W of 0.5. The initial crack were introduced by fatigue pre-cracking and EDM cutting with a wire of 0.1 mm thickness, which gave slits of 0.12 mm width. After fatigue pre-cracking all specimens were 20% side-grooved.

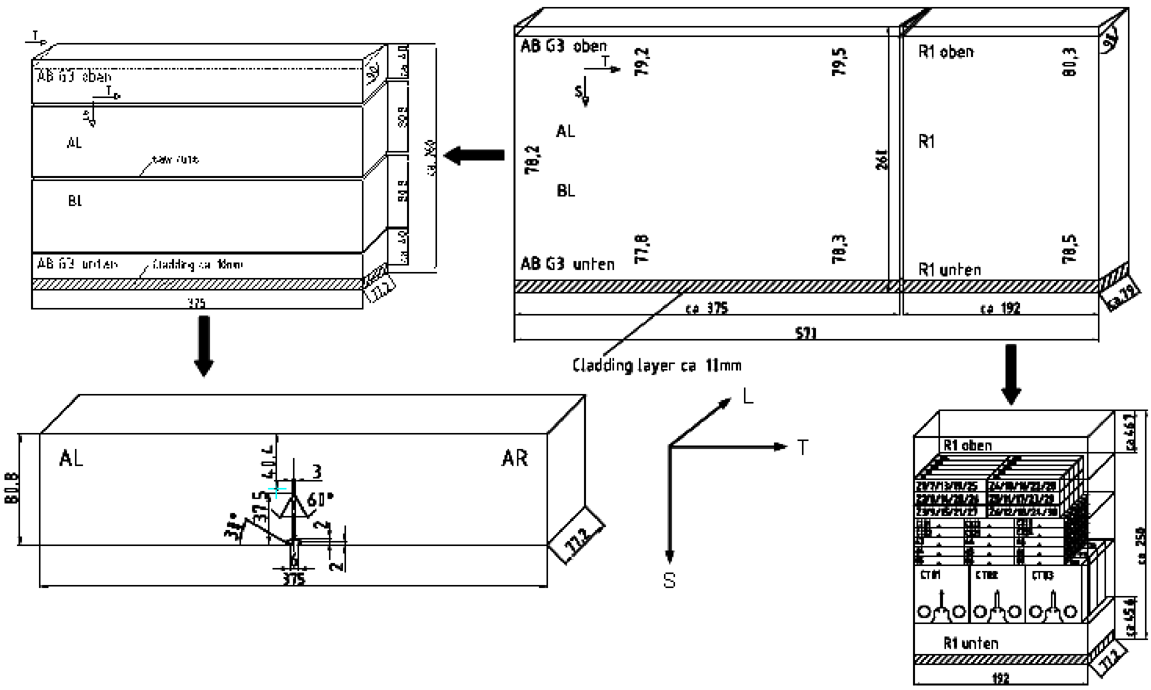

Figure 4.2: Sampling steps from block to SE(B) and 1T-C(T) specimens and the geometry of a 3T-SE(B) specimen.

5. Testing scheme and evaluation

Beside basic characterisation (microstructural analyses, quasi-static and dynamic tensile tests and impact tests) quasi-static MC tests (0.1 to 2 MPa√m/s, evaluated according to ASTM E1921-09a) and dynamic MC tests (up to 350000 MPa√m/s, evaluated according to HSK-AN-425 and an alternative approach, a combination of ISO/FDIS 26843 and ASTM E1921-09a) were conducted.

5.1 Tensile tests

In total 30 cylindrical tensile specimens of 8 mm diameter and 30 mm or 40 mm gage length machined according to [DIN 50125] were tested. They were T orientated according to [ASTM E 1823] and X oriented according to [ISO 3785]. Most of the tests were conducted in quasi-static displacement control (1 mm/min = 0.01667 mm/s = 17 MPa/s) at room temperature according to DIN EN 10002-1 and for elevated temperatures according to DIN EN 10002-5. A wide temperature range between -150 °C and +288 °C was covered to examine the temperature dependence of the tensile properties.

A number of specimens were tested between -40°C and +50°C at the following elevated loading rates to examine the velocity-dependence of the tensile properties:

60 mm/min = 1 mm/s = 1094 MPa/s
300 mm/min = 5 mm/s = 2170 MPa/s
900 mm/min =15 mm/s = 17835 MPa/s.

In most cases at least 2 samples were tested for each temperature and velocity.

The dynamic tensile properties for evaluating dynamic MC tests were not inferred from those tests but instead from the instrumented impact tests of the MC tests as mentioned below.

5.2 Charpy-V tests

Charpy-V tests were conducted on 30 Charpy-V specimens (10 mm x 10 mm x 55 mm) which were T-S oriented according to ASTM E 1823 and X-Z oriented according to [ISO 3785]. The tests were performed with an instrumented pendulum striker PSd 300 according to DIN EN 10045-1 and DIN EN ISO 14556. Temperature was controlled by liquid nitrogen bath and electrical heating. The test conditions were the following:
initial impact energy 300 J,
initial impact velocity 5.5 m/s and
temperature range -80 °C to + 275 °C.

5.3 Master Curve tests

Table 4.2 gives an overview over all conducted MC tests.

Table 4.2: Overview over MC tests

	v (setpoint)	v in m/s (actual value)	specimen type	crack configuration a/W ratio, fatigue/EDM	average dK/dt in MPa√m/s*
quasist.	0.2 mm/min		0.4T-SE(B)	0.5, fatigue+EDM	1.4
	”		“	0.3, fatigue+EDM	1.5
	”		0.8T-SE(B)	0.5, fatigue	1.0
	0.5 mm/min		1.6T-SE(B)	0.5, fatigue	1.7
	”		3T-SE(B)	0.5, fatigue	1.2
	0.25 mm/min		1T-C(T)	0.5, fatigue+EDM	1.0
	0.2 mm/min		0.5T-C(T)	0.5, fatigue	1.2
medium	0.10 m/s	0.04 m/s	0.8T-SE(B)	0.5, fatigue	11400
	“		0.4T-SE(B)	0.5, fatigue	16100
dynam.	1.2 m/s	1.2 m/s	0.4T-SE(B)	0.5, fatigue	149966
	“	“	“	0.5, EDM	157062
	2.4 m/s	2.4 m/s	“	0.3, fatigue	307248
	“	“	“	0.3, EDM	349392

* dK/dt for quasistatic and medium velocity tests was calculated according to ASTM E1921 via ΔLL/dt, and for dynamic tests as the average of the individual test series according to equation (29) in guideline HSK-AN-425 Rev. 5.

5.3.1 Quasistatic Master Curve testing

All quasi-static Master Curve MC reference temperatures T_0 were evaluated by applying the multitemperature option of ASTM E1921-09a as outlined briefly in Section 2. The temperature dependence of the applied Young's modulus was calculated from test results obtained from [MPA-06] which examined the same RPV steel (22 Ni MoCr 3-7 Biblis C). A least square linear fit leads to:

$$E(T) = -0.0585 \cdot T + 212.028 \quad (in\ GPa, T\ in\ °C, \quad -150°C \leq T \leq 150°C) \qquad (19)$$

Eq. (19) was used to calculate $K_{Jc(limit)}$ according to Eq. (6). The corresponding equation for the quasi-static 0.2% offset yield strength for the evaluation of quasi-static MC tests is given in section 6.1, Eq. (36).
Benchmark tests to evaluate the quasi-static reference temperature T_0 were performed on standard 0.4T-SE(B) specimens, fatigue pre-cracked to a/W=0.5 and subsequently 20% side-grooved. Further quasistatic MC tests were conducted on SE(B) specimens of different sizes (B=0.8T, 1.6T and 3T), with shorter cracks (a/W=0.3), and on 1T-C(T) specimens (a/W=0.5 only). Moreover, in most cases not only pre-cracked specimens were tested but also EDM notched specimen sets.

5.3.2 Impact Master Curve testing

For impact MC tests only 0.4T-SE(B) specimens can be used. Four different configurations were examined: short (a/W=0.3) and standard (a/W=0.5) crack length ratios, both either with fatigue pre-cracks or EDM machined notches. The fatigue-pre-cracked specimens were tested mostly at loading rates of 1.2 m/s while the EDM notched specimens were tested at 2.4 m/s. The dynamic MC reference temperature T_{0d} was calculated with two different evaluation methods, according to HSK-AN-425 [HSK-AN-425], abbreviated “HSK”, and according to ISO/FDIS 26843 combined with ASTM E1921, abbreviated “ISO/ASTM”.

In general, first the total fracture energy W_c from the start of the test (s=0, F=0) to the point instable failure (displacement s_c, force F_c) is calculated from the force-displacement plot as the area integral, Eq. (20).

$$W_c = \int_0^{s_c} F \cdot ds \qquad (20)$$

Then, by subtracting the elastic part from W_c the plastic part W_{cp} is found.

$$W_{cp} = W_c - \frac{F_c^2}{2 \cdot k(a = a_0)} \qquad (21)$$

In this formula, the slope of the force-displacement signal is not assessed individually by linear regression analysis unlike required by other test standards for instrumented impact testing. Instead, it the stiffness k is calculated with Eqs. (22) and (23), which are given as follows:

$$k(a) = \frac{E \cdot \left(2B \cdot B_N - B_N^2\right) \cdot (W - a)^2}{B \cdot S^2 \cdot (1 - \nu^2) \cdot g(a/W)} \qquad (22)$$

where E is entered in MPa, specimen thickness B, net thickness B_N, specimen width W, initial crack length or EDM notch length a and span S in mm, Poisson ratio v is dimensionless, and g(a/W) according to Eq. (23)

$$g(a/W) = 1.193 - 1.980 \cdot \left(\frac{a}{W}\right) + 4.478 \cdot \left(\frac{a}{W}\right)^2 - 4.443 \cdot \left(\frac{a}{W}\right)^3 + 1.739 \cdot \left(\frac{a}{W}\right)^4 \qquad (23)$$

Then, from W_{cp} the plastic part of the J-Integral J_{cd}, J_p, is calculated according to Eq. (24) and (25) while the elastic part J_e is calculated from stress intensity factors, Eqs. (26)-(28).

$$J_p = \frac{\eta(a) \cdot W_{cp}}{B_N \cdot (W - a)} \qquad (24)$$

$$\eta(a) = 1.857 + 0.143 \cdot (a / W) \qquad (25)$$

$$J_e = \frac{K_I^2(F_c, a)}{E} \cdot (1 - \nu^2) \qquad (26)$$

in which

$$K_I = \frac{F \cdot S}{\sqrt{B \cdot B_N \cdot W^3}} \cdot f\left(\frac{a}{W}\right) \qquad (27)$$

where F in N; a, S, B, B_N and W in mm, E in MPa, and

$$f\left(\frac{a}{W}\right)=\frac{3\cdot\sqrt{a/W}}{2\cdot\left(1+2\cdot\frac{a}{W}\right)\cdot\left(1-\frac{a}{W}\right)^{\frac{3}{2}}}\cdot\left(1.99-\frac{a}{W}\cdot\left(1-\frac{a}{W}\right)\cdot\left(2.15-3.93\cdot\frac{a}{W}+2.7\cdot\left(\frac{a}{W}\right)^{2}\right)\right) \quad (28)$$

Finally, the dynamic J-Integral J_{cd} is defined as the sum of J_e and J_p of Eqs. (24) and (26).

$$J_{cd} = J_e + J_p \quad (29)$$

T_0 is calculated with J_{cd} according to ASTM E1921-09a as described in Section 2.4.

According to the guideline draft (HSK-AN-425 Rev 5) only those specimens are used to calculate T_0 which either failed purely elastic (fracture type I), or at rising force with no prior load decrease (fracture type II). Regarding fracture type I, the HSK-AN-425 approach and the ASTM approach differ in how to calculate J_{cd}. Following HSK-AN-425, the plastic part J_p is omitted for specimens failing with fracture type I, Eq. (30), whereas in ASTM E1921 J_c always consists of an elastic and a plastic part, Eq. (29).

$$J_{cd} = J_e \quad (30)$$

Accordingly, for fracture type I the HSK evaluation always yields lower J_{cd} results than the ISO/ASTM evaluation scheme. Obviously, when a MC test batch consists of many specimens which failed with fracture type I and no or only few with fracture type II, the differences in T_0 calculated with HSK-AN-425 and with ISO/ASTM are most pronounced. Regarding fracture type II, the two evaluation methods are the same. J_{cd} consists of both elastic and plastic parts, J_e and J_p, Eq. (29).

At this evaluation stage, some additional aspects which are typical for dynamic testing might or might not be taken into account. Some (but not all) standards or draft standards for instrumeted impact tests recommends subtracting machine and/or specimen compliance from the energy values. Three correction methods were examined, abbreviated as follows:

- "ISO/ASTM-1": Irrespective of fracture type, all specimens' energy values are compliance corrected, but without including W_{pl}. The latter is what HSK requires for evaluating fracture type I specimens. Compliance is defined as:

$$C = C_M + C_S \quad (31)$$

  where

  C_M is the compliance of the testing apparatus measured on the applied impact pendulum as $1.81\cdot10^{-9}$ m/N and

  C_S is the compliance of the specimen calculated as $3.79\cdot10^{-9}$ m/N.

- "ISO/ASTM-2": Without any compliance corrections, but W_{pl}. is included in all energy calculations, including fracture type I. This option is the most similar to the ASTM approach.

- "ISO/ASTM-3": With compliance correction according to choice 1, but this time contains W_{pl} for all specimens.

Because HSK-AN-425 Rev. 5 corrects the raw data not for machine compliance but for specimen compliance only and because it is easier to compare dynamic and quasistatic T_0 if not another parameter (with/ without W_{pl}) is introduced for specimens of fracture type I, "ISO/ASTM-2" was chosen to be the prime evaluation procedure for dynamic MC tests.

Once the dynamic J_{cd} values from several specimens are known, they are processed further according to ASTM E1921-09a as given in Section 2.4. From J_{cd} the plane strain K_{Jcd} is calculated, then normalized to a virtual specimen thickness of 1T and solved iteratively for reference temperature T_0, Eq. (10).

After Joyce [Joyce-98] and Yoon [Yoon-02] demonstrated a very strong and systematic influence of the loading rate on T_0, ASTM E1921 was limited to quasi-static loading rates of maximum 2 MPa√m/s. Yet, a simple formula has just entered the latest version of ASTM E1921-09 through which the dynamic T_{0d} can be roughly estimated from a known quasi-static T_0 [Wallin-97], Eqs. (32) and (33). In these formulae T_{0d} is named "$T_{0,Xest}$" but for the sake of coherence will be labelled "$T_{0,d}^{est}$" in this report.

$$T_{0,d^{est}} = \frac{(T_0 + 273.15) \cdot \Gamma}{\Gamma - \ln(X)} - 273.15 \qquad (32)$$

where X = dK/dt in MPa√m/s and temperature is in °C.
The function of Γ is given by:

$$\Gamma = 9.9 \cdot \exp\left[\left(\frac{T_0 + 273.15}{190}\right)^{1.66} + \left(\frac{\sigma^{T_0}_{YS)}}{722}\right)^{1.09}\right] \qquad (33)$$

where σ_{YS}^{T0} is the yield strength measured or estimated at T_0 and at quasi-static rates (~ 10^{-6} to 10^{-4} s^{-1}). These formulae were developed on 59 steels with σ_{YS} = 200 to 1000 MPa quasi-static yield strength, dK/dt = 10^{-1} to 10^{6} MPa√m/s, and T_0 = -180 to 0 °C.
The dynamic 0.2% yield strength σ_d is considerably higher than the quasi-static one. Thus, in order to calculate K_{Jc} and $K_{Jc(limit)}$ correctly, σ_d should be known, preferably its temperature dependence, too. It was semi-empirically derived as follows: All dynamically tested 0.4T-SE(B) specimens with a/W=0.5 fatigue pre-crack, tested at 1.2 m/s (dK/dt=1.5*10^{6} MPa√m/s), which showed a distinct general yield force F_{gy} were used as input in Eq. (33), which originates from [Server-1978] but was corrected for European DIN/ISO striker tup radii of 2 mm, [Richter-1999].

$$\sigma_d = \frac{4F_{gy}}{C \cdot B_N \cdot (W-a)^2} \cdot \frac{S}{4} = \frac{C' \cdot F_{gy}}{B \cdot (W-a_0)^2} \cdot \frac{S}{4} \qquad (34)$$

Eq. (34) is valid for Charpy size SE(B) specimens with fatigue pre-cracks. Interestingly, according to [Richter-99] the constraint factor, C', of 3.13 for specimens with fatigue-precracks is hardly different from 3.14 for non cracked ones.
The dynamic yield strength used in the MC evaluation according to ASTM E1921-09a is calculated according to Eq. (34) using the load at general yield determined from the load deflection traces of the respective tests. From these ($\sigma_{d;T}$) data points, the temperature dependence was found to follow a simple linear regression fit, Eq. (35).

$$\sigma_d(T) = -1.6398 \cdot T + 730.9 \qquad (35)$$

6. Results

6.1 Tensile tests

The formula for Young's Modulus for both quasi-static and dynamic testing is given in Eq. (19). The temperature dependence for quasi-static 0.2% offset yield strength follows a simple exponential curve, Eq. (36) in Figure 6.1.1.

$$\sigma_{YS}(T) = 349 + 86.7 \cdot \exp(-0.00691 \cdot T) \quad in\ MPa \qquad (36)$$

The tensile properties also depend on loading rate, Fig. 6.1.2.

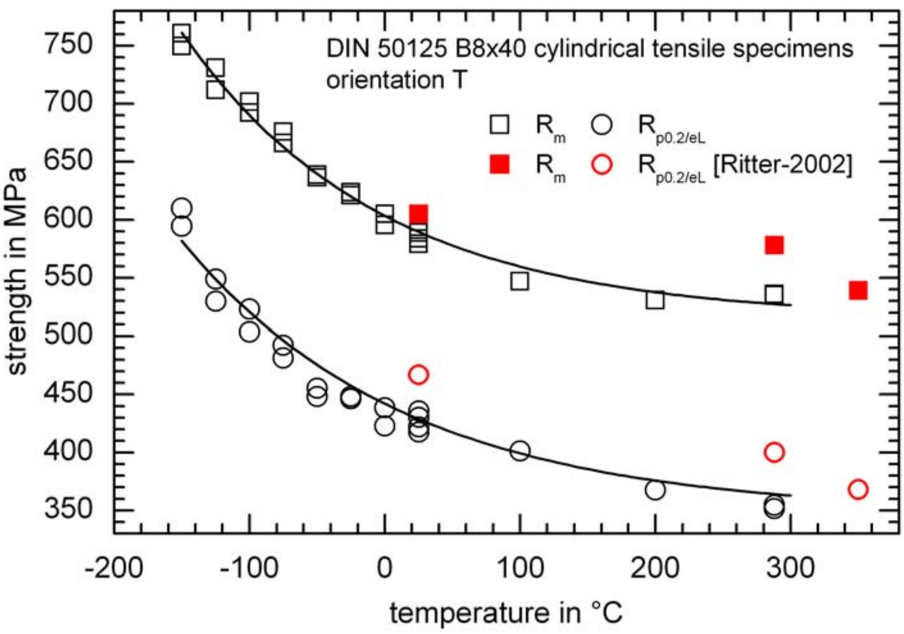

Fig. 6.1.1: Influence of temperature on quasi-static tensile properties σ_{YS} and UTS

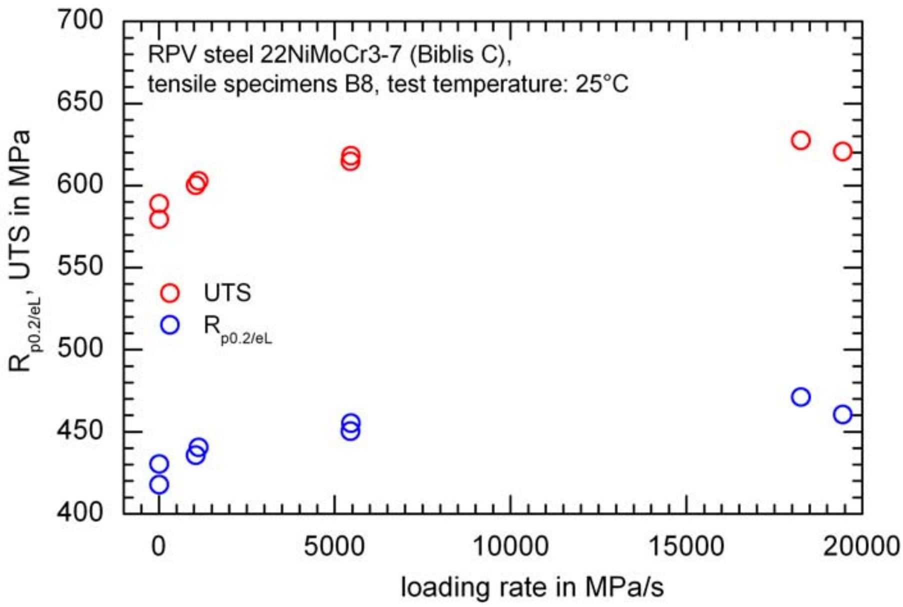

Fig. 6.1.2: Influence of loading rate on tensile properties σ_{YS} and UTS

6.2 Charpy-V tests

Ductile-to-brittle transition curves and the properties deducted from them like upper shelf energy (USE) and transition temperatures at specific values of absorbed impact energy (T_{28J}, T_{41J}, T_{48J}, T_{68J}) are important aids in characterizing the irradiation induced ductile-to-brittle transition shift of RPV steels in the present indirect and correlative integrity assessment codes. Figure 6.2.1 shows the ductile-to-brittle transition curve and the tanh fit curve parameters.

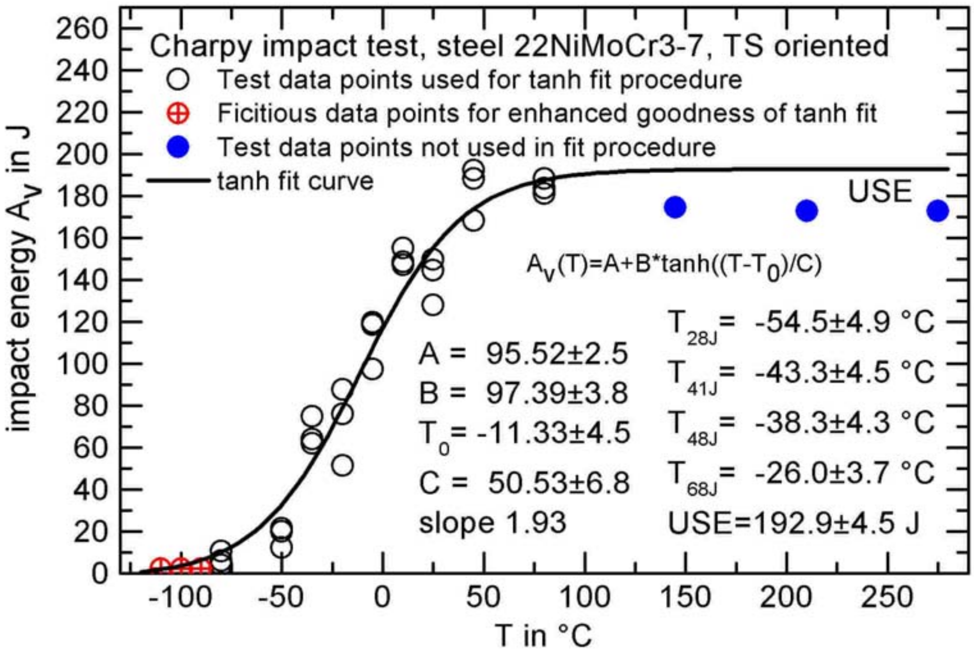

Figure 6.2.1: Charpy-V impact energy transition curve

6.3 *Master Curve Tests*

The majority of the MC tests were conducted at temperatures in the validity window according to ASTM E 1921-09a, a few also on higher temperatures to study the behaviour in the upper transition range. Scanning Electron Microscopy (SEM) fractographs with varying magnifications were taken to cover all areas from whole specimen halves down to micron scale near crack initiation sites.

Figure 6.3.1 to Figure 6.3.3 show typical fractographic images of a specimen which failed with comparatively high K_{Jc} values (1T-C(T) specimen “CT14”, high test temperature T_{test} = -26°C, high $K_{Jc(1T)}$ = 246.3 MPa√m). Figure 6.3.4 and Figure 6.3.5 show an example of a specimen which failed at quite low K_{Jc} values (1T-C(T) specimen “CT16”, low test temperature T_{test} = -116°C, low $K_{Jc(1T)}$ = 70.4 MPa√m). For both examples, several magnification levels are given, gradually zooming in on the crack initiation point (Figures 6.3.1 and 6.3.2 for specimen CT14, Figures 6.3.4 and 6.3.5 for specimen CT16). In both cases the crack does not initiate directly at the fatigue crack front but at a certain distance ahead of the crack tip, inside the ligament. These results support the weakest link theory, which is one of the cornerstones of the MC concept. It states that the crack initiates at a weak spot inside the whole stressed volume in front of the crack tip, which doesn’t necessarily need to be situated directly at the crack.

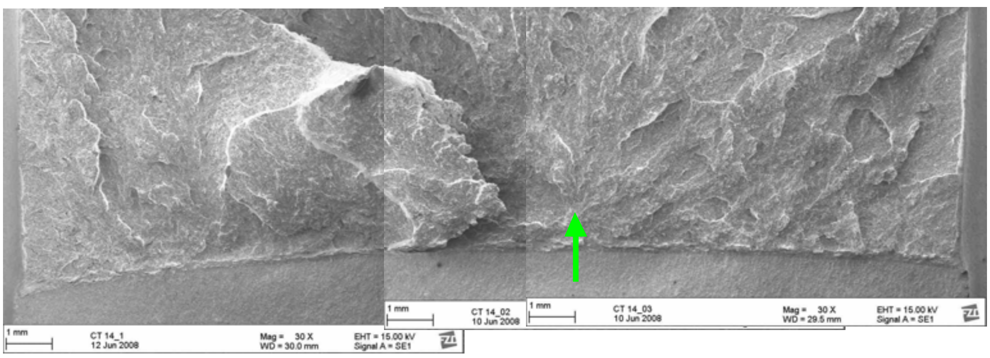
Figure 6.3.1: Fracture surface of specimen „CT14“, arrow indicating the crack initiation site.

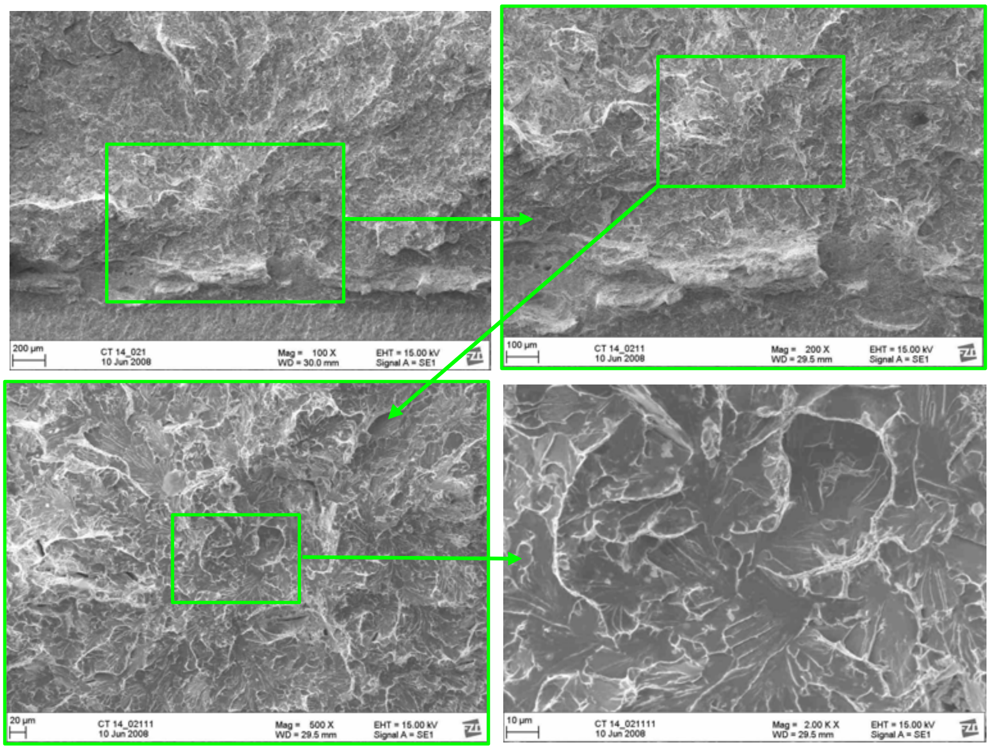

Figure 6.3.2: Crack initiation site of specimen „CT14” in 100-, 200-, 500- and 2000-fold magnification

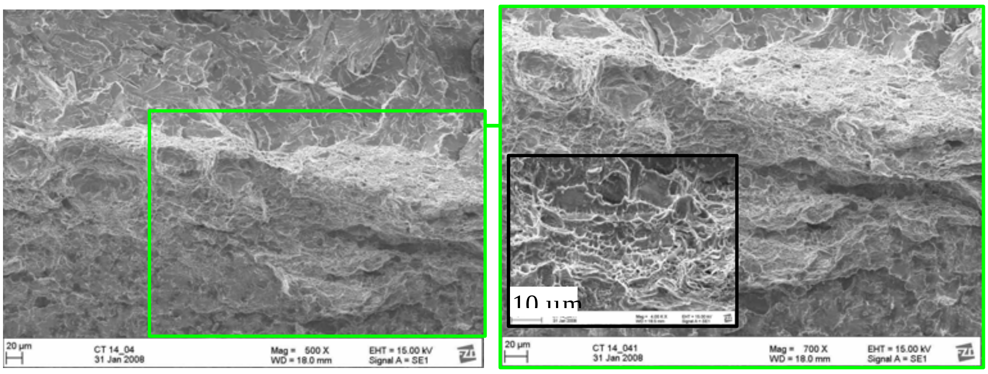

Figure 6.3.3: Ductile crack initiation - dimples along the fatigue crack front of specimen „CT14”

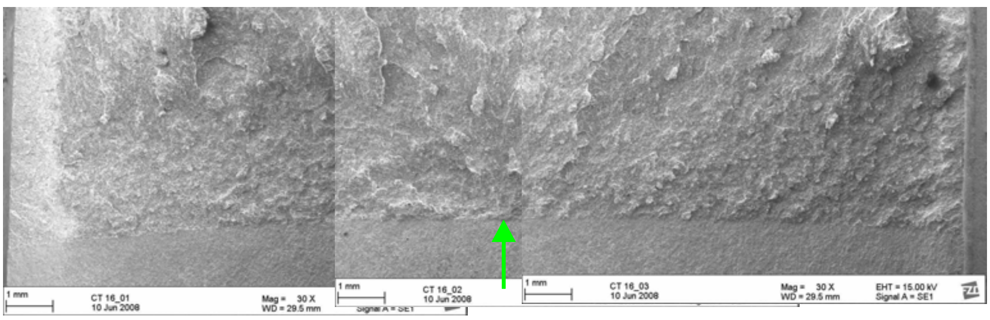

Figure 6.3.4: Fracture surface of specimen „CT16“, arrow indicating the crack initiation site.

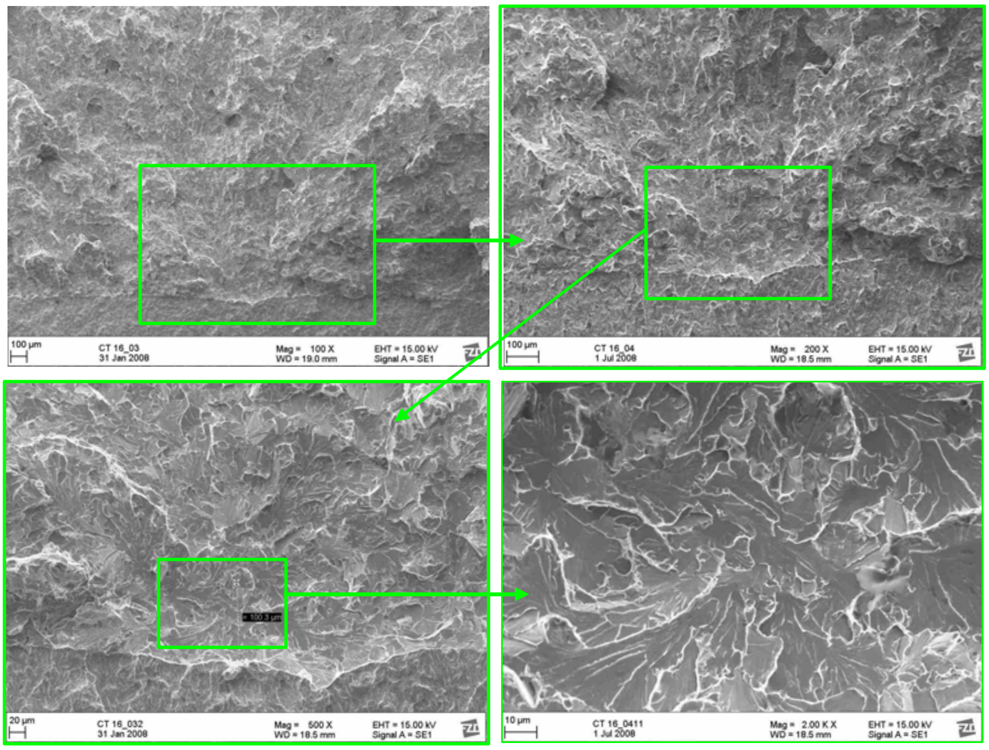

Figure 6.3.5: Crack initiation site of specimen „CT16" in 100-, 200-, 500- und 2000-fold magnification.

Transcrystalline cleavage was observed on all analysed fracture surfaces as shown by the two examples. Figure 6.3.3 shows the ductile crack initiation before cleavage failure. Ductile dimples are visible along the fatigue crack front, which is typical for specimens which failed at high toughness values. Occasionally MnS inclusions were found at either crack initiation sites or on the fatigue pre-cracked surface but their occurrence did not lead to particularly low toughness results.

6.3.1 Influence of specimen size on the reference temperature T_0

SE(B) specimen batches of different thickness with B=0.4T, 0.8T, 1.6T and 3T (side grooves are not considered) were tested. The results are summarised in Table 6.3.1 and depicted in Fig. 6.3.6. For the assessment of the influence of the specimen size on T_0 only specimens tested at temperatures close to the expected T_0 ($T_0 \pm 20$ K) are considered in Table 6.3.1. Table 6.3.1 also contains the T_0 evaluated with all tested SE(B) specimens with which the Master Curves in Fig. 6.3.6 are indexed. This joint evaluation results in a T_0 of -80.3°C. However, the differences of the other specimens sizes except the 1.6T SE(B) specimens lie within the 1σ scatter band. Obviously, the 1.6T SE(B) specimens yield higher T_0. Note that from the highest thickness T = 3T only four specimens could be machined, too few to be evaluated properly with ASTM E1921-09a in which minimum six specimens are required.

Table 6.3.1: Influence of specimen thickness on quasi-static MC T_0 (specimens with fatigue-precracks to a/W=0.5 and 20% side-grooves, tested at temperatures within T_0 ± 20 K).

specimen thickness B in T (1T=25.4mm)	Master Curve evaluation (ASTM E1921-09a)					Loading rate	
	T_0 °C	σ K	$\Sigma r_i n_i$ -	r -	N -	$\frac{\Delta LL}{dt}$ mm/min	$\frac{dK}{dt}$ MPa√m/s
0.4	-83.0	6.4	2.07	13	16	0.2	1.38
0.8	-85.9	7.0	1.67	10	11	0.2	0.96
1.6	-71.6	7.5	1.33	8	8	0.2	0.96
3	n.a.	n.a.	n.a.	0	4	0.5	1.10
all SE(B) specimens (0.4 to 3)	-80.3	4.9	6.57	42	63	0.2; 0.5	see above

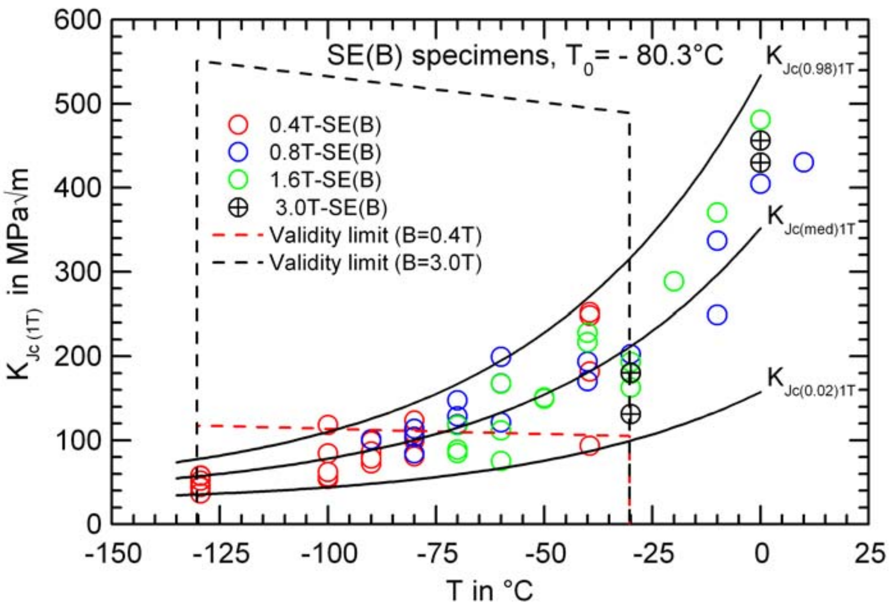

Fig. 6.3.6: Influence of the thickness B on quasi-static T_0 (dK/dt= 0.96 to 1.70 MPa√m/s) of fatigue pre-cracked (a/W=0.5) and 20% side-grooved SE(B) specimens.

One reason for the higher T_0 of the 1.6T SE(B) specimens can be seen in the low K_{Jc} measuring capacity, Eq. (6) of the smaller specimens compared to the larger specimens. In ASTM 1921-09a the constraint factor M is 30 for which relatively large loss of constraint is predicted in different investigations [IWM-2005, Server-2009, Tregoning-2000]. As seen in Fig. 6.3.6 many of the tested 0.4-T-SE(B) specimens are close to or above $K_{Jc(limit)}$. The larger specimens show an increasing $K_{Jc(limit)}$ as depicted in Fig. 6.3.6 Specimens with a thickness larger than 1T when tested around T_0 do not suffer the loss of constraint at their reported K_{Jc} values, unlike the 0.4T-and 0.8T-SE(B) specimens. The trend to higher T_0 with increasing specimen thickness has also been reported elsewhere [Server-2009].
The fracture toughness curves (MC) in Figure 6.3.6 are indexed with T_0=-80.3°C evaluated with the K_{Jc} values of the SE(B) specimens (B = 0.4T to 3T). The $K_{Jc(1T)}$ values of the tested SE(B) specimens with different thickness and of the 1T-C(T) specimens lie within the 0.02 and the 0.98 fractiles of cumulative fracture probability. Even the 1.6T-SE(B) and 1T-C(T) specimens which gave higher T_0 are enveloped by the 0.02 and the 0.98 fractiles.

6.3.2 Influence of specimen type on the reference temperature T_0

As given in Table 6.3.2 the T_0 evaluated with the K_{Jc} values measured on all 0.4T-SE(B) and 1T-C(T) specimens are -82.0°C and -74.0°C, respectively, which gives an offset of 8 K. The result is graphically depicted in Fig. 6.3.7. If only the specimens tested at temperatures in the range of around T_0 ± 20K are evaluated the offset accounts 12 K. The 0.5T-C(T) specimens tested at temperatures in the range of around T_0 ± 20K gave an offset of 7.7 K. As shown in Table 6.3.2 the differences in T_0 of the C(T) specimens are within one standard deviation. The difference in T_0 of 10 to 15 K between SE(B) and 1T-C(T) specimens as mentioned in the test standard ASTM E1921-09a was observed in the result, with the present maximum difference beeing 12 K. With increasing number of specimens the degree of accuracy of T_0 is higher. The difference between the evaluation of all SE(B) specimens (Table 6.3.1) and all C(T) specimens (Table 6.3.2) is 6 K.

Table 6.3.2: Influence of specimen type on quasi-static MC T_0 (specimens with fatigue-precracks of a/W=0.5 and 20% side-grooves, tested at temperatures within T_0 ± 20 K).

specimen B in T (1T=25.4mm)	Master Curve evaluation (ASTM E1921-09a)					Loading rate	
	T_0 °C	σ K	$\Sigma r_i n_i$ -	r -	N -	$\frac{\Delta LL}{dt}$ mm/min	$\frac{dK}{dt}$ MPa√m/s
0.4T-SE(B)*	-83.0	6.4	2.07	13	16	0.2	1.38
0.4T-SE(B)**	-82.0	6.3	2.24	14	28	0.2	1.38
1T-C(T)*	-71.0	7.5	1.33	8	8	0.25	1.04
1T-C(T)**	-74.0	5.6	3.21	21	21	0.25	1.04
0.5T-C(T)*	-75.3	7.2	1.43	9	9	0.2	1.20
1T and 0.5T-C(T)*	-73.4	5.9	2.76	17	17	0.2,0.25	1.2, 1.04
1T and 0.5T-C(T)**	-74.3	5.2	4.64	30	30	0.2,0.25	1.2, 1.04

* test temperatures T_0 ± 20 K; ** all tested specimens

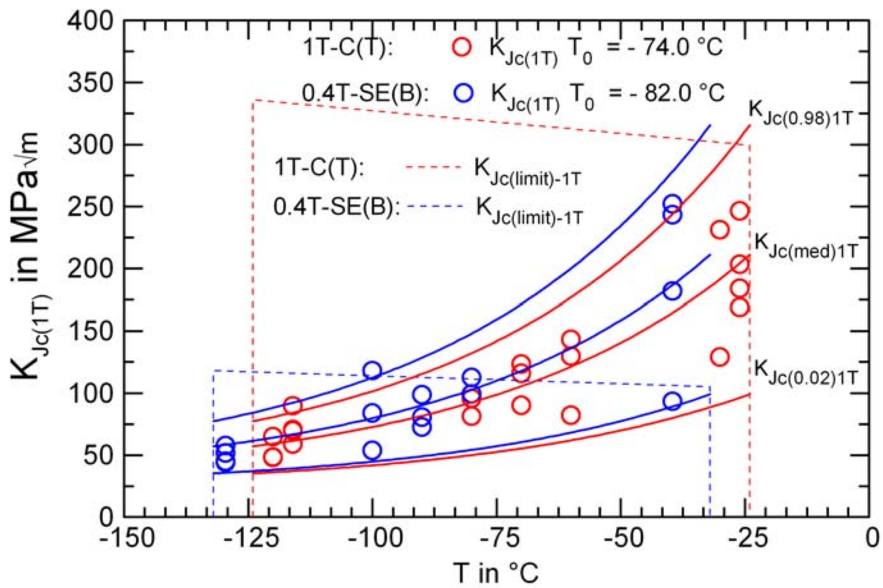

Fig. 6.3.7: $K_{Jc(1T)}$ values and MC measured on 1T-C(T) and 0.4T-SE(B) specimens (fatigue pre-cracked a/W=0.5 and 20% side-grooved).

6.3.3 Influence of test temperature on the reference temperature T_0

Table 6.3.3 summarizes the T_0 evaluation in dependence of the test temperature measured on 0.4T-SE(B) and 1T-C(T) specimens (pre-cracked at a/W=0.5 and 20% side-grooves). The inclusion of the specimens tested close to the limits of the temperature range T_0 ± 50 K influences the evaluated T_0. For 0.4T-SE(B) and 1T-C(T) specimens there is a maximum difference of 21.8 K and 10.0 K, respectively. As shown in Table 6.3.3 there is no systematic influence of the test temperature on T_0. Whereas 0.4T-SE(B) gave remarkably higher T_0 when the K_{Jc} values close to the limits of the temperature range are considered, whereas the 1T-C(T) show the opposite trend. The 1T-C(T) specimens tested 48 K below the T_0 gave approximately about 10 K lower T_0. For the quantisation it has to be taken into account that the number of 0.4T-SE(B) and 1T-C(T) specimens is different and 3 out of 4 0.4T-SE(B) specimens tested at T_0 +43 K are censored. Additionally, the T_0 of -61.2°C (Table 6.3.3) evaluated with 0.4T SE(B) specimens tested at -130°C is not valid, because the test temperature is outside the validity range of ± 50 K. For comparison test results of an IAEA CRP programme show on the contrary lower T_0 evaluated with specimens tested at test temperature near T_0 -50 K [Server-2005b]. It can be finally stated that except for the lowest test temperature allowed by ASTM E1921-09a, the different T_0 values are very consistent. However, the testing in the temperature range of T_0 ± 20 K is recommended, because it gave the highest accuracy.

Table 6.3.3: Influence of test temperature on quasi-static MC T_0 (specimens with fatigue pre-cracks of a/W=0.5 and 20% side-grooves).

specimen B in T (1T=25.4mm)	T	Master Curve evaluation (ASTM E1921-09a)					Loading rate	
		T_0	σ	$\Sigma r_i n_i$	r	N	$\frac{\Delta LL}{dt}$	$\frac{dK}{dt}$
	°C	°C	K	-	-	-	mm/min	MPa√m/s
0.4T-SE(B)	close T_0	-83.0	6.4	2.07	13	16	0.2	1.38
0.4T-SE(B)	close T_0 & +43 K	-82.0	6.3	2.24	14	20	0.2	1.38
0.4T-SE(B)	close T_0 & -47 K	-78.8	6.4	2.07	13	24	0.2	1.38
0.4T-SE(B)	all	-82.0	6.3	2.24	14	28	0.2	1.38
0.4T-SE(B)	T_0 -47 K	-61.2	-	0.00	0	8	0.2	1.38
1T-C(T)*	close T_0	-71.0	7.5	1.33	8	8	0.25	1.04
1T-C(T)*	close T_0 & +43 K	-70.7	6.3	2.33	14	14	0.25	1.04
1T-C(T)	close T_0 & -48 K	-75.5	6.1	2.21	15	15	0.25	1.04
1T-C(T)	all	-74.0	5.6	3.21	21	21	0.25	1.04
1T-C(T)	T_0 -48 K	-80.7	7.9	0.88	7	7	0.25	1.04
1T-C(T)	T_0 +43 K	-70.4	8.4	1.00	6	6	0.25	1.04

6.3.4 Influence of crack length ratio a/W on the reference temperature T_0

Fatigue pre-cracked specimens with a/W=0.3 and a/W=0.5 crack lengths yield comparable T_0, Table 6.3.4. Short crack specimens (a/W=0.3) yield T_0 = -76.3°C ± 6.8 K ($\Sigma r_i n_i$ = 1.12, N = 7, r = 7), while SE(B) specimens with a/W=0.5 yield T_0 = -83.0 °C ± 6.4 K ($\Sigma r_i n_i$ = 2.07, N = 16, r = 13). Both 1σ scatter bands overlap. This behaviour is not expected from the theory, since the crack-tip constraints in terms of Q or T are significantly lower in the case of a/W=0.3. The lower constraint would yield to higher K_{Jc} values and so to lower T_0, which is opposite to the trend measured here. Similar results were found in [IWM-2005], in which MC specimens from the same RPV vessel batch and the same orientation TS were tested, Table 6.3.4.

Table 6.3.4: Influence of crack length ratio on quasi-static T_0 (ASTM E1921-09a) of fatigue-precracked and 20% side-grooved 0.4T-SE(B) specimens.

a/W	T_0 ±1σ	reference
	°C	
0.50	-83.0 ± 6.4	
0.50	-76.3	[IWM-2005, Fig. 4.9a]
0.30	-76.3 ± 6.8	
0.18	-76.0	[IWM-2005, Fig. 4.9b]
≈0.13	-92.7	[IWM-2005, Fig. 4.9c]

According to [IWM-05] even a/W - ratios as low as 0.18 have no effect on the reference temperatures, Table 6.3.4. Only at very low crack length ratios of a/W≈0.13, which correspond essentially to plane stress, a decrease in T_0 was obtained. From these unexpected results it can be concluded that the constraints in 0.4T-SE(B) specimens are not much dependent on crack-length for a/W > 0.18. Thus, it can be concluded that either the constraint is already fully developed in specimens with quite shallow cracks of just a/W=0.18, or more likely that the initial constraints have decayed to about the same amount at the longer cracks as in the case of shorter crack at cleavage initiation. Only at very low crack length ratios of a/W≈0.13 an increase of the effective fracture toughness and the corresponding decrease of T_0 was observed. Instead of plane strain conditions now plane stress conditions prevail in front of the crack tip due to slip-line fields between the crack-tip and the surface in the wake of the crack. On the other hand the results based on 0.4T-SE(B) specimens tested at temperature close to T_0 give K_{Jc} values which are close to the $K_{Jc(limit)}$, hence the influence of the rather low M factor in Eq. (6) can not be excluded.

The experimental results published in [IWM-2005] were conducted in order to verify the outcomes of comprehensive nonlinear finite element simulations in which the effects of specimen type, specimen size and crack length on T_0 were analyzed thoroughly. The results from the experiments and numerical simulations correlate very well, both qualitatively and quantitatively. Deviations are small, in most cases within the 1σ scatter band of the experiments. Therefore it can be concluded that the surveillance specimens of the Swiss NPP from the 1970ies with shorter crack lengths (a/W=0.3) than prescribed by ASTM E1921 (0.45<a/W<0.55) may still be used for the determination of reliable T_0 reference temperatures.

6.3.4 Replacement of fatigue cracks with EDM notches

Table 6.3.5 summarizes the T_0 calculated with K_{Jc}-values measured with specimens tested in the temperature range of the expected T_0 and calculated with the multimodal option of ASTM E1921-09a. The T_0 of EDM notched specimens lies 44 K to 54 K below the T_0 of fatigue pre-cracked specimens. This shift in T_0 is universally true for SE(B) and C(T) specimens and examined testing conditions. Figure 6.3.8 shows a typical example of how the Master Curve shifts to lower temperatures when using EDM notches rather than pre-fatigue cracks. This result agrees with results of a Charpy impact test round robin [Boehme - 2002], where the shift between fatigue cracked and EDM notched Charpy size impact specimens was 40 K.

Table 6.3.5: Influence of crack/notch configuration on T_0.

specimen type	a/W	loading rate	$T_{0[d]}$ crack °C	$T_{0[d]}$ EDM notch °C	ΔT_0 K
1T-C(T)	0.5	quasi-static	-71.0	-119.1	48.1
0.4T-SE(B)	0.3	quasi	-76.3	-129.9	53.6
0.4T-SE(B)	0.5	quasi	-83.0	-129.3	46.3
0.4T-SE(B)	0.5	dynamic (1.2 m/s)	-11.7	-55.7	44.0

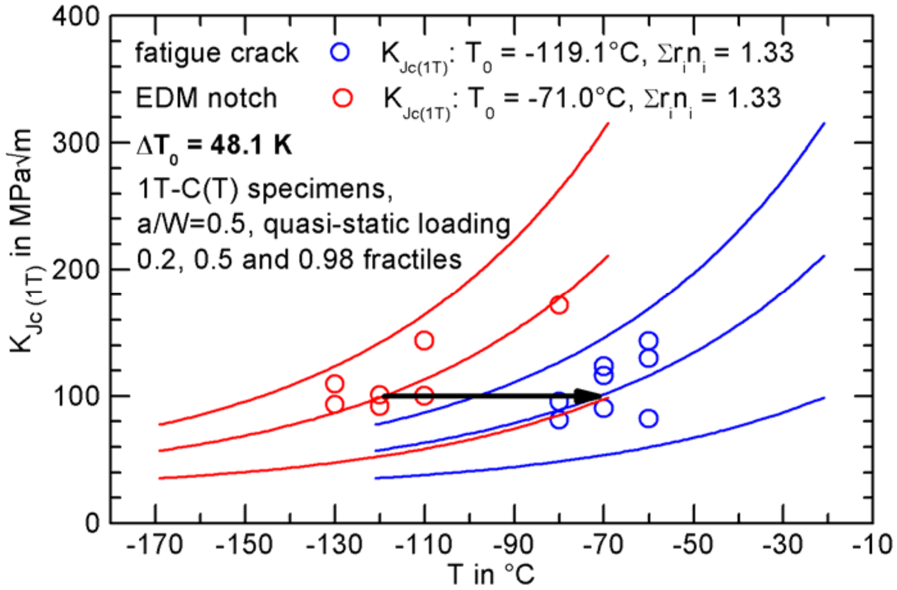

Fig. 6.3.8: Influence of the crack configuration in the 1T-C(T) specimens on T_0 and Master Curves.

6.3.5 Influence of loading rate (quasi-static vs. dynamic) and evaluation method on the reference temperature T_0

By increasing the loading rate from quasi-static to dynamic, the T_0 is shifted by up to 78 K for specimens with a/W=0.5, (dynamic pendulum hammer velocity 1.2 m/s) and 69 K for specimens with a/W=0.3 (2.4 m/s), Table 6.3.6. The Master Curves of all 0.4T-SE(B) specimens with a/W=0.5 are shown in Figure 6.3.9. The large T_0 shifts agree with results from other labs. In the literature shifts between quasi-static and dynamic loading were found to be between 52 and 88 K [IWM-2005, Viehrig-2002, Server-2009] depending on the loading rate.

Table 6.3.6: Influence of loading rate on MC T_0 (fatigue pre-cracked and 20% side-grooved SE(B) specimens).

Specimen type	loading rate	X=dK/dt	σ_{YS}^{T0}	T_0, T_{0d}, $T_{0d,est}$	ΔT	Evaluation method
		MPa√ms^{-1}	MPa	°C	K	
0.4T-SE(B), a/W=0.5 (1.2 m/s)	quasi-static	1	506.2	-86.1	0	ASTM E1921-09a
	dynamic	16100	506.2	-28.2	57.9	ASTM E1921-09a
	impact	150000	506.2	-7.7	78.4	HSK-AN-425
	impact	150000	506.2	-11.7	74.4	“ISO/ASTM-2”
	impact	150000	506.2	-30.1	56.0	Eq. (28)
0.4T-SE(B), a/W=0.3 (2.4 m/s)	quasi-static	1	495.9	-76.3	0	ASTM E1921-09a
	medium	-	-	-	-	ASTM E1921-09a
	impact	300000	495.9	-7.5	68.8	HSK-AN-425
	impact	300000	495.9	n.a.*	-	“ISO/ASTM-2”
	impact	300000	495.9	-18.5	57.8	Eq. (28)
0.8T-SE(B), a/W=0.5	quasi-static	1	505.9	-85.8	0	ASTM E1921-09a
	dynamic	11400	505.9	-32.5	53.3	ASTM E1921-09a

* weighting sum 0.83<1, thus no valid T_0 according to ASTM E1921

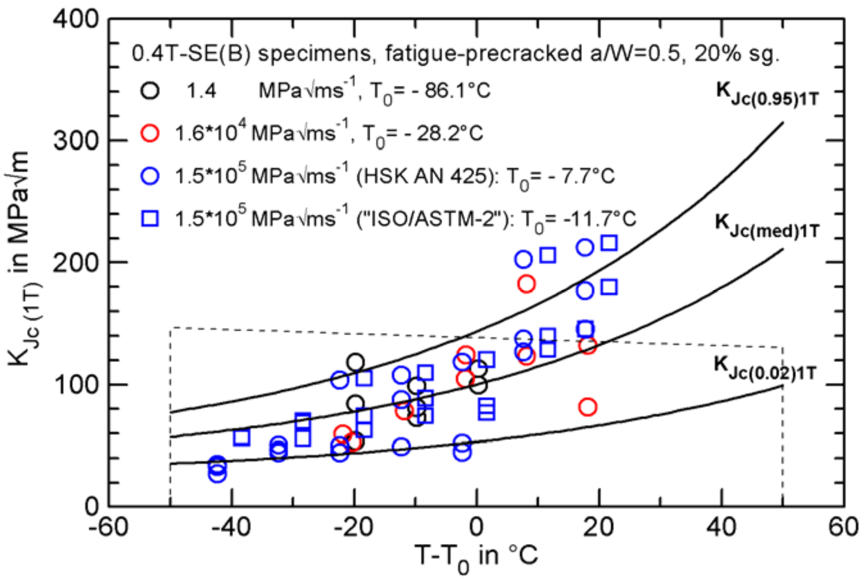

Figure 6.3.9: Influence of loading rate on the MCs of fatigue pre-cracked 0.4T-SE(B) specimens, a/W=0.5, K_{Jc} values adjusted to T_0 of the test series.

Table 6.3.4 shows that the choice of the evaluation method is not very important. Comparing the two different methods of evaluating dynamic MC test data, the HSK-AN-425 evaluation yields a 4 K higher T_0 temperature than the modified ASTM E1921 procedure "ISO/ASTM-2", as was to be expected for reasons explained in Section 5.3.2. Furthermore, Table 6.3.6 illustrates that the proposed prediction formula Eq. (32) under-predicts $T_{0,d}$ in comparison with the experimental results. Figure 6.3.10 shows the relation between actually achieved experimental T_0 results and predicted T_0 results. The estimated $T_{0,d}$ values deviate from the experimentally obtained $T_{0,d}$ by 22 K (a/W=0.5) and 11 K (a/W=0.3). Input variables used in Eq. (32) are given in Table 6.3.7.

Table 6.3.7: Input data for Eqs. (32) and (33)

a/W	Quasistatic T_0	X=dK/dt	σ_{YS}^{T0}
-	°C	MPa√m /s	MPa
0.5	-86.1	150000	506.2
0.3	-76.3	300000	495.9

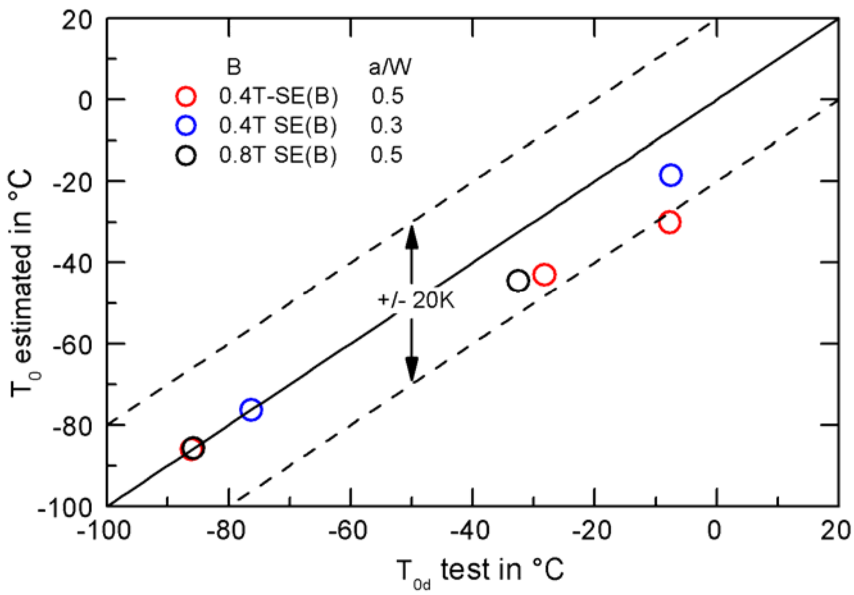

Figure 6.3.10: Goodness of fit of experimental $T_{0,d}$ results and estimated $T_{0,d}^{est}$ results, both evaluated according to ASTM E1921-09a.

6.3.6 Statistical analyses of the cleavage fracture toughness values

The measured K_{Jc} values are converted to the corresponding values at their respective reference temperatures (T_0). The conversion is performed by moving a particular K_{JC} value to the respective reference temperature (T_0) along its fractile curve (P_f = const) in the following manner [Nagel 2006]:

1. MC at the temperature T equals:

$$K_{Jc}(T) = [11 + 77 \cdot \exp(0.019 \cdot (T - T_0)] \cdot (LN(1 - P_f))^{1/4} + K_{\min} \quad (37)$$

2. MC at the temperature $T=T_0$ equals:

$$K_{Jc}(T = T_0) = 88 \cdot (-LN(1 - P_f))^{1/4} + K_{\min} \quad (38)$$

3. The re-arrangement of Eq. (37) by substitution of $(-LN(1-P))^{1/4}$ from Eq. (38) results in:

$$K_{Jc}(T = T_0) = \frac{K_{\min} + 88 \cdot (K_{Jc}(T) - K_{\min})}{11 + 77 \cdot \exp(0.019 \cdot (T - T_0))} \quad (39)$$

Statistical analyses show that the converted $K_{Jc(1T)}$ data have a normal distribution clustering around a mean of 99 MPa√m which is very close to the theoretical value of 100 MPa√m (Figure 6.3.11). The straightness of the probability density function and the symmetrical bell-shaped distribution of the values around the mean also implies that the MC concept approach is applicable.

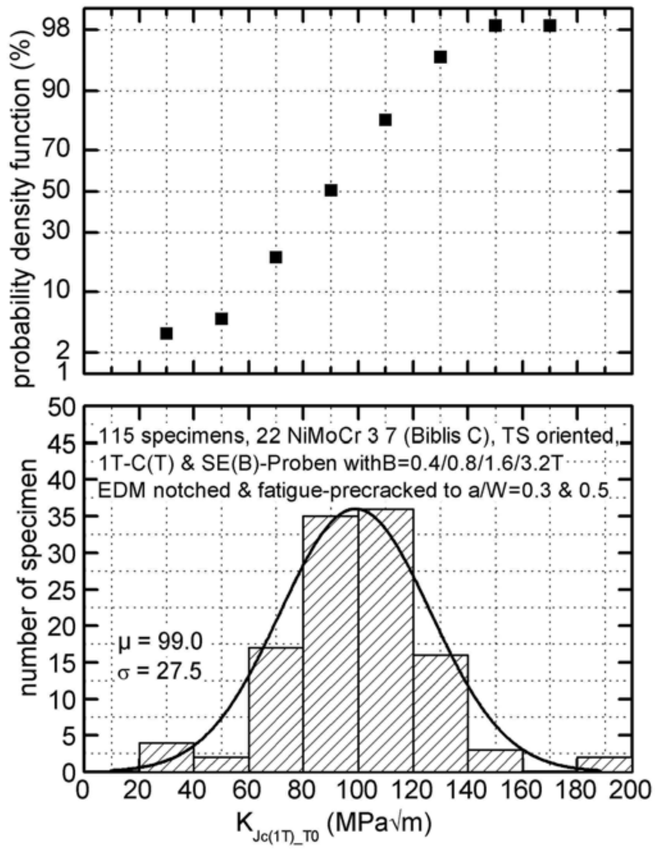

Fig. 6.3.11: Probability density function (above, in%) and histogram (below) of the converted $K_{JC(1T)}$ of quasi-statically tested specimens

6.4 *Application of the Master Curve Test Results in the Reactor Pressure Vessel Integrity Assessment*

Figure 6.3.12 shows the 1T size adjusted fracture toughness values $K_{Jc(1T)}$ measured on SE(B) specimens of different size, 0.5T-C(T) and 1T-C(T) specimens. The Figure also depicts the ASME K_{IC} reference curves (Eq. (12)), indexed to RT_{To}, Eq. (13), and RT_X, Eqs. (15) and (16). RT_{To} is calculated with the T_0 measured with following specimens (Tables 6.3.1 and 6.3.2):

- 0.4T-SE(B) specimens: RT_{To} = -80.3°C + 19.4 K = -60.9°C according to Eq. (13),
- 0.4T-SE(B) specimens: RT_X = -80.3°C + 55 K = -25.3°C according to Eq. (15),
- 1T-C(T) specimens. RT_{To} = -74.0°C + 19.4 K = -54.6°C according to Eq. (13) and
- 1T-C(T) specimens: RT_{To} = 74.0°C + 40 K = -34.0 °C according to Eq. (16).

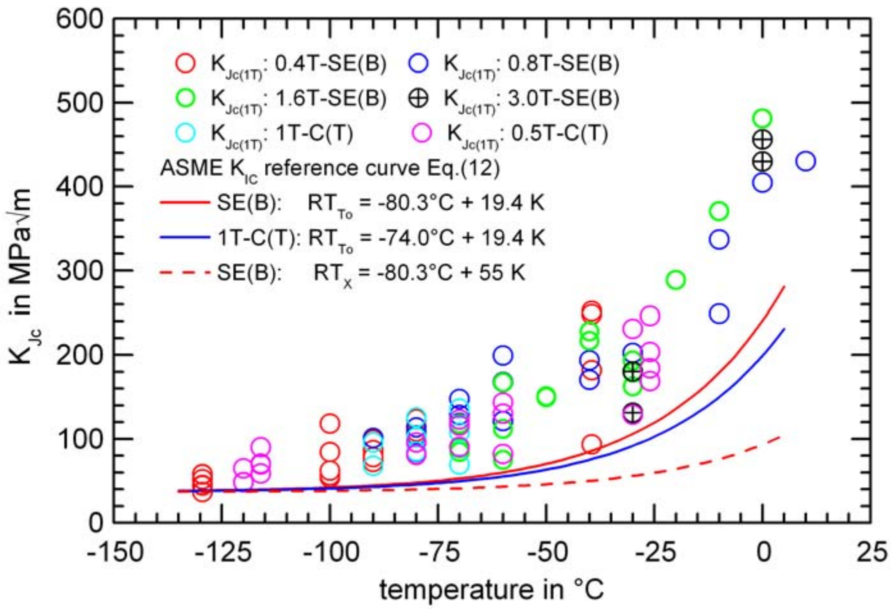

Fig. 6.3.12 $K_{Jc(1T)}$ values 1 T size adjusted measured on SE(B) and 1T-C(T) specimens and ASME-K_{IC} reference curve indexed to RT_{To} according to ASME N-629 and RT_x according to ENSI-B01/d.

It should be taken into account that the primary ASME-K_{IC} reference curve reflects K_{IC} values determined according to ASTM E399 which are non-size adjusted according to ASTM E1921-09a, Eq. (2). The reference temperature RT_{To}, Eq. (13), as specified in the ASME Code Case N-629 [ASME N-629] is based on T_0 calculated with size adjusted $K_{Jc(1T)}$ values, therefore the corresponding ASME-K_{IC} reference curve should envelop the measured $K_{Jc(1T)}$ values. As depicted in Fig. 6.3.12 all $K_{Jc(1T)}$ values lie above the ASME-K_{IC} reference curve indexed to RT_{To} -60.9°C, which was evaluated with all tested SE(B) specimens. Even the $K_{Jc(1T)}$ values measured on 1T-C(T) specimens which gave approximately 6 K higher T_0 are enveloped by that curve. The ASME-K_{IC} reference curve indexed to RT_{To} -54.6°C evaluated with all tested 1T-C(T) specimens envelops all $K_{Jc(1T)}$ values with a margin. The ENSI draft guideline [ENSI-B01/d] recommends higher margins of 40 K and 55 K for Charpy size 0.4T-SE(B) and 1T-C(T) specimens, respectively. As demonstrated in Fig. 6.3.12 these margins are rather conservative, hence the dashed curve envelops the $K_{Jc(1T)}$ values comfortably.

Fig. 6.3.13 shows the same data, without the data being size adjusted to 1T. One K_{Jc} value of a 3T-SE(B) specimens is shown to slightly transgress the RT_{To}-indexed K_{IC} curve. Without size adjustment the fracture toughness data from larger specimens shift to lower fracture toughness values than the 1T-adjusted data. In the reports [Rosinski-1999, Server -2000] concerning the basics of the ASME Code Case N-629 [ASME N-629] the key point is the degree of bounding of the K_{Jc} data rather than the specimen size. Data points below the ASME-K_{IC} reference curve are considered to be acceptable as long as the number is consistent with a 5% lower tolerance bound [Server-2000]. This is the case for the one data point right of the RT_{To} ASME-K_{IC} reference curve in Fig. 6.3.13. An additional argument why this one data point is considered to be acceptable is the large crack-front length of 3T (77 mm). This size is significantly larger than any real flaws that could go undetected in a reactor pressure vessel.

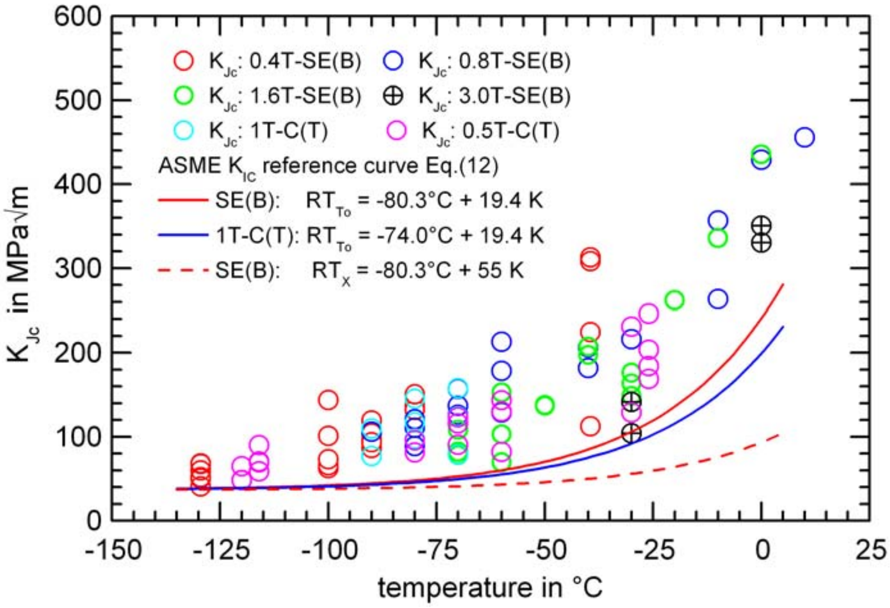

Fig. 6.3.13 K_{Jc} values without 1 T size adjustment measured on SE(B) and 1T-C(T) specimens and ASME-K_{IC} reference curve indexed to RT_{To} according to ASME N-629 and RT_x according to ENSI-B01/d.

7. Summary and conclusions

The objectives of the investigations presented in this paper are to assess some issues which are in discussion regarding the application of the Master Curve approach in nuclear reactor pressure vessel integrity assessment.

- The applicability of pre-cracked 0.4T-SE(B) specimens with cracks shorter than usual (a/W=0.3 instead of a/W=0.5) is investigated.
- The transferability of MC reference temperatures from 0.4T thick specimens to larger specimens had to be verified.
- Furthermore, the influence of the specimen type and the test temperature on the reference temperature is ascertained.
- The applicability of specimens with electroerosive notches for the fracture toughness testing is assessed.
- Also, the influence of the loading rate and specimen type on the Master Curve reference temperature T_0 should be quantified.

The following main results are ascertained and conclusions can be drawn:

1. SE(B) specimens with different overall sizes (specimen thickness B=0.4T, 0.8T, 1.6T, 3T, fatigue pre-cracked to a/W=0.5 and 20% side-grooved) have comparable T_0. T_0 varies within the 1σ scatter band. This validates the specimen size scaling procedure of test standard ASTM E1921 and affirms the transferability of results from tests on 0.4T Charpy size SE(B) specimen to larger one's.
2. The testing of C(T) specimens results in higher T_0 compared to SE(B) specimens. Depending on the number of specimens and the test temperature range the maximum offset is determined with 12 K. With the increasing number of specimens the degree of

accuracy of T_0 is higher. The evaluation of all pre-cracked SE(B) and C(T) specimens (a/W=0.5, 20% side grooved) tested over the whole temperature range of T_0 ± 50 K results in an offset of 6 K.

3. It can be stated that except for the lowest test temperature allowed by ASTM E1921-09a, the T_0 values evaluated with specimens tested at different test temperatures are consistent. The testing in the temperature range of T_0 ± 20 K is recommended, because it gave the highest accuracy.
4. Specimens with a/W=0.3 and a/W=0.5 crack length ratios yield comparable T_0. An other research group which tested specimens of the same steel found that at even shorter crack length ratios of a/W=0.18 the specimens exhibit T_0 comparable to that of a/W=0.5 specimens. The constraint conditions break down and T_0 start to differ significantly in specimens with very shallow cracks of a/W=0.13. Thus it can be concluded that pre-cracked 0.4T-SE(B) specimens with shorter than usual crack sizes of a/W=0.3 provide the same K_{Jc} values as the 0.4T-SE(B) specimens with a/W=0.5, and are therefore equally eligible for fracture toughness characterization.
5. The T_0 of EDM notched specimens lie 44 K up to 54 K below the T_0 of fatigue pre-cracked specimens. This effect is observed both in specimens of different thickness (0.4T and 0.8T), with different loading rates (quasi-static and dynamic), in both SE(B) and C(T) specimen types and with different crack length ratios (a/W=0.5 and 0.3).
6. A significant influence of the loading rate on the MC T_0 was observed. Increasing the loading rate from quasi-static to dynamic, T_0 increases for specimens with a/W=0.5 by 78 K (dK/dt=150000 MPa√m/s) and for specimens with a/W=0.3 by 69 K (dK/dt=300000 MPa√m/s). An estimation formula proposed in ASTM E1921-09a to predict the dynamic $T_{0,d}$ from the quasi-static T_0 value differs from the experimentally obtained values by up to 22 K. It is explicitly mentioned in ASTM E1921-09a that such a bias of up to 20 K may exist. Thus, this formula is appropriate for determining an initial test temperature for dynamic tests, but shall not be used for calculating and reporting values of reference temperatures corresponding to elevated loading rates as mentioned in ASTM E1921-09a.
7. HSK AN 425 is a suitable method to evaluate dynamic MC tests. The $T_{0,d}$ results differs by only 4 K from the result obtained with the “ISO/ASTM-2” evaluation method, mainly arising from the different approaches of treating specimens which fail in a very brittle manner. For these specimens we suggest to include the plastic energy, W_p, in the J integral of the HSK AN 425 evaluation, like it is common in other fracture mechanics test standards like ASTM E 1820 and ASMT E1921.
8. The reference temperature T_0 is eligible to define a reference temperature RT_{To} for the ASME-K_{IC} reference curve as recommended in the ASME Code Case N-629. An additional margin has to be defined for the specific type of transient to be considered in the RPV integrity assessment and which also takes into account the level of available information of the RPV to be assessed.

Acknowledgement

This study was funded by the Swiss Federal Nuclear Inspectorate (Research Project No. H100456).

References

ASME NB-2300: American Society for Mechanical Engineers, Rule for construction of nuclear power plants. ASME Boiler and Pressure Vessel Code, Sect. III: Rep.. ASME NB-2300, ASME, New York, 2002.

ASME N-629: American Society of Mechanical Engineers: Use of Fracture Toughness Test data to Establish Reference Temperature for Pressure Retaining Materials, Section XI, Division1, ASME Boiler and Pressure Vessel Code Case N-629, ASME, New York, 1999.

ASTM E399-09: Standard Test Method for Linear-Elastic Plane-Strain Fracture Toughness K_{Ic} of Metallic Materials, ASTM International, 2009.

ASTM E 1823-09a: Standard Terminology Relating to Fatigue and Fracture Testing , ASTM International, Version 2009a.

ASTM E1921-09a: Standard Test Method for Determination of Reference Temperature, T0, for Ferritic Steels in the Transition Range, ASTM International, 2009.

Boehme-2002: Boehme, W.: Results of a DVM Round Robin on Instrumented Charpy Testing, From Charpy to Present Testing, ESIS Publication 30, D. Francois and A. Pineau (Eds.), Elsevier, 2002, pp. 189-196.

Brumovsky-2001: Brumovsky, M.: Master Curve application to embrittled RPVs of WWER type reactors. Proc. of the ASME Pressure Vessel and Piping Conference 2001, American Society of Mechanical Engineers, New York, 2001.

CASTOC-04: Crack Growth Behaviour of Low Alloy Steel for Pressure Boundary Components under Transient Light Water Reactor (LWR) Operating Conditions. Project Reference FIKS-CT-2000-00048. European Community 5th Framework Programme (1998-2002), 2004.

DIN EN 10002-1: Metallische Werkstoffe - Zugversuch - Teil 1: Prüfverfahren bei Raumtemperatur. Köln: Beuth, 2001-12.

DIN EN 10002-5: Metallische Werkstoffe; Zugversuch; Teil 5: Prüfverfahren bei erhöhter Temperatur. Köln: Beuth, 1992-02.

DIN EN 10045-1: Metallische Werkstoffe; Kerbschlagbiegeversuch nach Charpy; Teil 1: Prüfverfahren. Köln: Beuth, 1991-04.

DIN EN ISO 14556: Stahl - Kerbschlagbiegeversuch nach Charpy (V-Kerb) - Instrumentiertes Prüfverfahren (ISO 14556:2000 + Amd.1:2006) Köln: Beuth, 2000 09 und 2006-10.

DIN 50125: Prüfung metallischer Werkstoffe – Zugproben. Köln: Beuth, 2004-01.

ENSI-2010: Richtlinie Alterungsueberwachung, Draft, Swiss Federal Nuclear Safety Inspectorate ENSI, ENSI-B01/d, January 2010.

ISO/FDIS 26843: Metallic materials – Measurement of fracture toughness of steels at impact loading rates using precracked Charpy specimens. Entwurf 2007-11-13 (ISO TC 164/SC4 N465.5, under development, FDIS registered for formal approval, Stand 06/09).

HSK-AN-425: Prüfrichtlinie HSK AN 425 Rev. 5, Verfahren zur bruchmechanischen Auswertung von instrumentierten Schlagbiegeversuchen an angerissenen Kerbschlagbiegeproben. HSK, 14. Aug. 2007.

IWM-2005: Abschlussbericht Vorhaben-Nr. 1501239: Kritische Überprüfung des Mastercurve-Ansatzes im Hinblick auf die Anwendung bei deutschen Kernkraftwerken. Berichts-Nr. S8/2004. Freiburg: Fraunhofer-Institut für Werkstoffmechanik, 2005.

ISO/FDIS 26843: ISO 26843, 2008-10, Metallic Materials - Measurement of Fracture Toughness of Steels at Impact Loading Rates using precracked Charpy Specimens, Draft Standard, International Organisation for Standardization.

ISO 3785: ISO 3785:2006 Metallic materials – Designation of test specimen axes in relation to product texture, International Organisation for Standardization.

Joyce-1998: Joyce, J. A.: On the Utilization of High Rate Charpy Test Results and the Master Curve to Obtain Accurate Lower Bound Toughness Predictions in the Ductile-to-brittle Transition, Small Specimen Test Techniques. In: Small Specimens Test Techniques, W. R. Corwin et. al. (Eds.), ASTM STP 1329, ASTM Intl., West Conshohocken, PA, ISBN-13: 978-0-8031-2476-9, 1998.

KTA 3201.2: Safety Standards of the Nuclear Safety Standards Commission (KTA), KTA 3201.2 (06/96) (incl. rectification from BAnz 129, 13.07.00): Components of the reactor coolant pressure boundary of light water reactors, Part 2: Design and Analysis. KTA-Geschaeftsstelle c/o Bundesamt fuer Strahlenschutz (BfS), Albert-Schweitzer-Strasse 18, 38226 Salzgitter, Germany.

KTA 3203: Safety Standards of the Nuclear Safety Standards Commission (KTA): KTA 3203 (6/01): Surveillance of the Irradiation behaviour of reactor pressure vessel materials of LWR facilities. KTA-Geschaeftsstelle c/o Bundesamt fuer Strahlenschutz (BfS), Albert-Schweitzer-Strasse 18, 38226 Salzgitter, Germany.

Mc Cabe-2005: Mc Cabe, D. E., Merkle J. G., Wallin K.: An introduction to the development and use of the Master Curve method. ASTM International, West Conshohocken, PA, USA, May 2005.

MPA-2006: Abschlussbericht Vorhaben-Nr. 1501240: Kritische Überprüfung des Masterkurve-Ansatzes im Hinblick auf die Anwendung bei deutschen Kernkraftwerken. Berichts-Nr. 8886 000 000. Stuttgart: Materialprüfungsanstalt Univ. Stuttgart, 2006.

Richter-1999: Richter, H.: Zur Problematik der Bestimmung dynamischer Festigkeitskennwerte im instrumentierten Kerbschlagbiegeversuch. Jahressitzung 1999 der DVM-Arbeitsgruppe „Instrumentierter Kerbschlagbiegeversuch“, 24.09.1999, TU BA Freiberg.

Ritter-2002: Ritter, S.; Seifert, H.P.: Charakterisation of lower shell and weld material of the Biblis C reactor pressure vessel. PSI Bericht Nr. 02-01, Paul Scherrer Institut, Villingen, Schweiz, Januar 2002.

Rosinski-1999, Rosinski, S.: Application of Master Curve Fracture Toughness Methodology for ferritic Steels (PWRMRP-01).

PWR Materials Reliability Project (PWRMRP), EPRI, Palo Alto, CA, USA: 1999TR-108390, Revision 1.

Rosinski-2000: Rosinski; S. T. Server, W. L.: Application of the Master Curve in the ASME Code. International Journal of Pressure Vessels and Piping, Volume 77, Issue 10 , 15 August 2000, pp. 591-598.

Rosinski-2004: Rosinski, S.: Materials Reliability Program: Implementation Strategy for Master Curve Reference Temperature, T0 (MRP-101) EPRI, Paolo Alta, CA and U.S. Department of Energy, Washington, D.C.:2004.1009543.

Server-2000: Server, W. L., Rosinski, S.T.: Thechnical basis for application of the Master Curve approach in reactor pressure vessel integrity assessment
Effects of Radiation on Materials: 19th International Symposium, ASTM STP 1366, M.L. Hamilton, A.S. Kulmar, S.T. Rosinsky, and M.L. Grossbeck, Eds., American Society for Testing and Materials, West Conshohocken, PA, 2000,pp. 127-142

Server-2005a: Server, W. L. et al.: IAEA Guidelines for Application of the Master Curve Approach to Reactor Pressure Vessel Integrity in Nuclear Power Plants
IAEA-Technical Reports Series 429, IAEA in Austria
March 2005.

Server-2005b: Server, W. L. et al.: Application of surveillance programme results to reactor pressure vessel integrity assessment; results of a coordinated research project 2000-2004, IAEA-TECDOC-1435, IAEA Aprill 2005

Server-2009: Server, B., et al: Master Curve Approach to Monitor Fracture Toughness of Reactor Pressure Vessels in Nuclear Power Plants, IAEA-TECDOC-1631, International Atomic Energy Agency, Vienna, 2009.

Tregoning-2000: Tregoning, R. L.; Joyce, J. A.: Investigation of Censoring Limits for Cleavage Fracture Determination, Fourth Symposium on Small Specimen Test Techniques, Reno, Nevada, USA, 23-25 January, 2000.
VERLIFE-2003: Brumovsky, M.: Unified Procedure for Lifetime Assessment of Component and piping in WWER NPPs "VERLIFE", European Commission, Final Report, Contract N° FIKS-CT-2001-20198, September 2003.

Nomenclature

a	crack length
B	specimen thickness
B_N	specimen net thickness between side grooves
b	ligament size b = W-a
B_{1T}	normalization specimen thickness 1T=25.4 mm
C	compliance
C	constraint factor
C'	=C/4; for Charpy size SE(B) specimens and ISO tup C' = 3.13
C_M	compliance of the testing apparatus measured on the applied impact pendulum with $1.81 \cdot 10^{-9}$ m/N and
C_S	compliance of the specimen calculated as $3.79 \cdot 10^{-9}$ m/N.
E	Young's modulus
F	load
F_c	load at cleavage failure of the specimen
J_c	$= J_e + J_p$
J_e	elastic part of the J integral
J_p	plastic part of the J integral
K_{Jc}	cleavage fracture toughness of the tested specimen
$K_{Jc(i)}$	individual $K_{Jc(1T)}$ value
$K_{Jc(limit)}$	validity limit for measured K_{Jc} (MPa√m)
$K_{Jc(med)1T}$	fracture toughness of a 1T specimen for a fracture probability of 50%
$K_{Jc(1T)}$	cleavage fracture toughness of a specimen with a thickness of B_{1T}
K_{min}	minimum fracture toughness fixed at 20 MPa√m in ASTM E1921-09a
K_0	scale parameter corresponding to 63.2% failure probability
K_I	fracture toughness at the load of cleavage failure of the specimen
K_{IC}	plain strain crack initiation reference fracture toughness
M	dimensionless size (constraint) criterion fixed at 30 in ASTM E1921-09a
N	number of tested specimens (valid K_{Jc} values)
n_i	specimen weighting factor for $T-T_0$ range i as shown in Table 4 of ASTM E1921-09a
P_f	failure probability
r	number of valid K_{Jc} values
r_i	number of valid specimens within $T-T_0$ range i
RT_{To}	reference transition temperature based on Master Curve (ASTM E1921-09a) T_0
S	span
T	test temperature (°C)
T_i	test temperature corresponding to $K_{Jc(i)}$ (°C)
T_0	Master Curve reference temperature (°C) at $K_{Jc(med)1T}$ = 100 MPa√m
W	specimen width
W_c	total fracture energy
W_{cp}	compliance corrected total fracture energy
Y	safety factor in the margin term

σ	margin in the VERLIFE procedure $\sigma = \sqrt{\sigma_1^2 + \delta T_M^2}$	
	σ_I	standard deviation according to ASTM E1921-09
	δT_M	considers the scatter in the materials; if this value is not available the application of the following values is suggested δT_M = 10°C for the base material, δT_M = 16°C for weld metals.
σ_{To}	uncertainty in the reference temperature T_0 in K	
$\sigma_{\phi t}$	uncertainty in the neutron fluence in K	
σ_{HT}	uncertainty in material heat treatement (non-homogeneity) in K	
σ_{YS}	yield strength at test temperature	
v	Poisson's ratio for steel (0.3)	
δ_i	censoring parameter: δ_i = 1 if the $K_{Jc(i)}$ datum is valid (Eq. (6)) or δ_i = 0 if the $K_{Jc(i)}$ datum is invalid and censored	